FROM MICROSCOPY TO NANOSCOPY

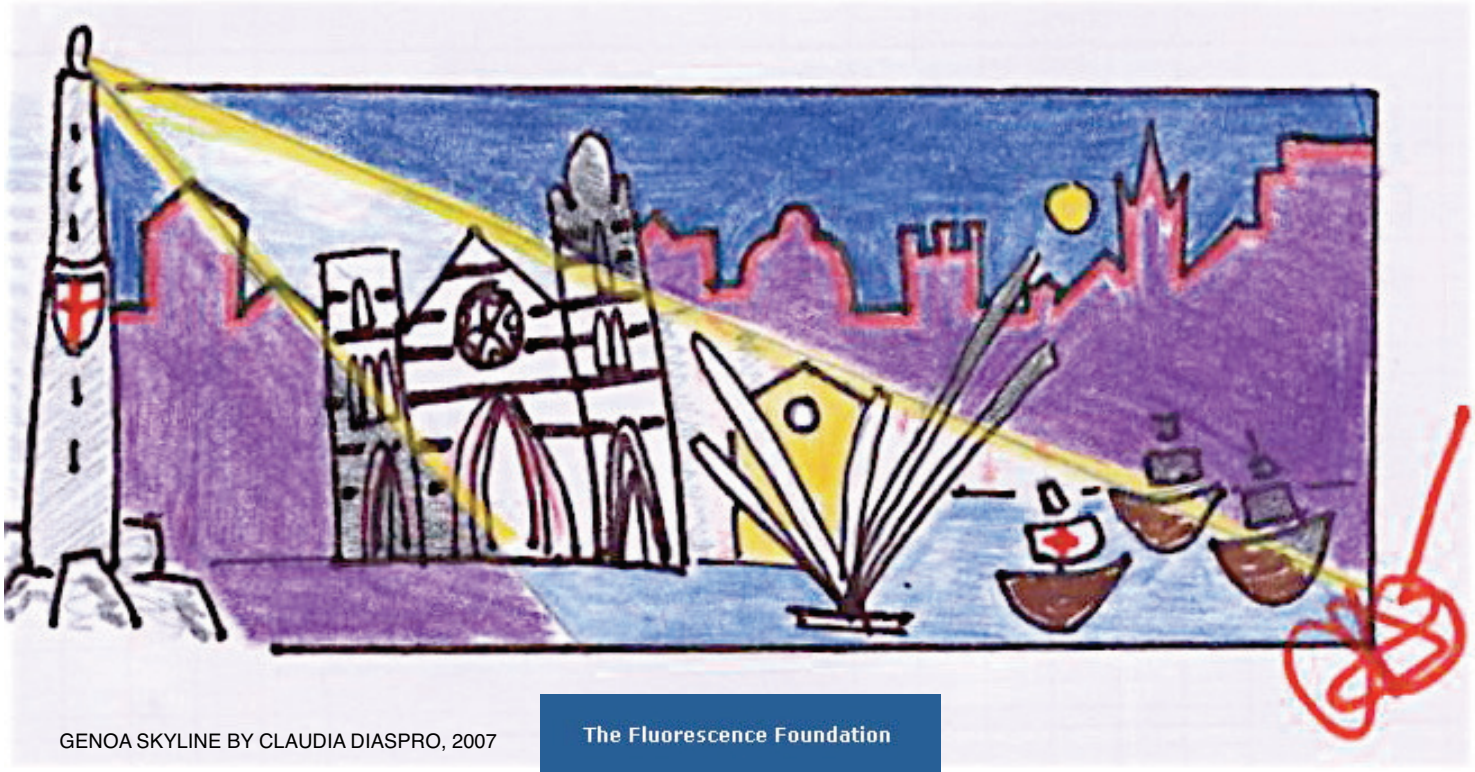

GENOA SKYLINE BY CLAUDIA DIASPRO, 2007

The Fluorescence Foundation

Department of Physics, University of Genoa
LAMBS, MicroScoBiO Research Center, IFOM

diaspro@fisica.unige.it
http://www.lambs.it

Alberto Diaspro

Alberto Diaspro
Cesare Usai
Paola Ramoino
Partha P. Mondal
Giuseppe Vicidomini
Paolo Bianchini
Valentina Caorsi
Davide Mazza
Ilaria Testa
Francesca Cella
Emiliano Ronzitti
Silke Krol
Raffaella Magrassi
Marc Schneider
Munish Chanana
Mattia Pesce
Federica Morotti
Francesco Di Fato
Mirko Corosu

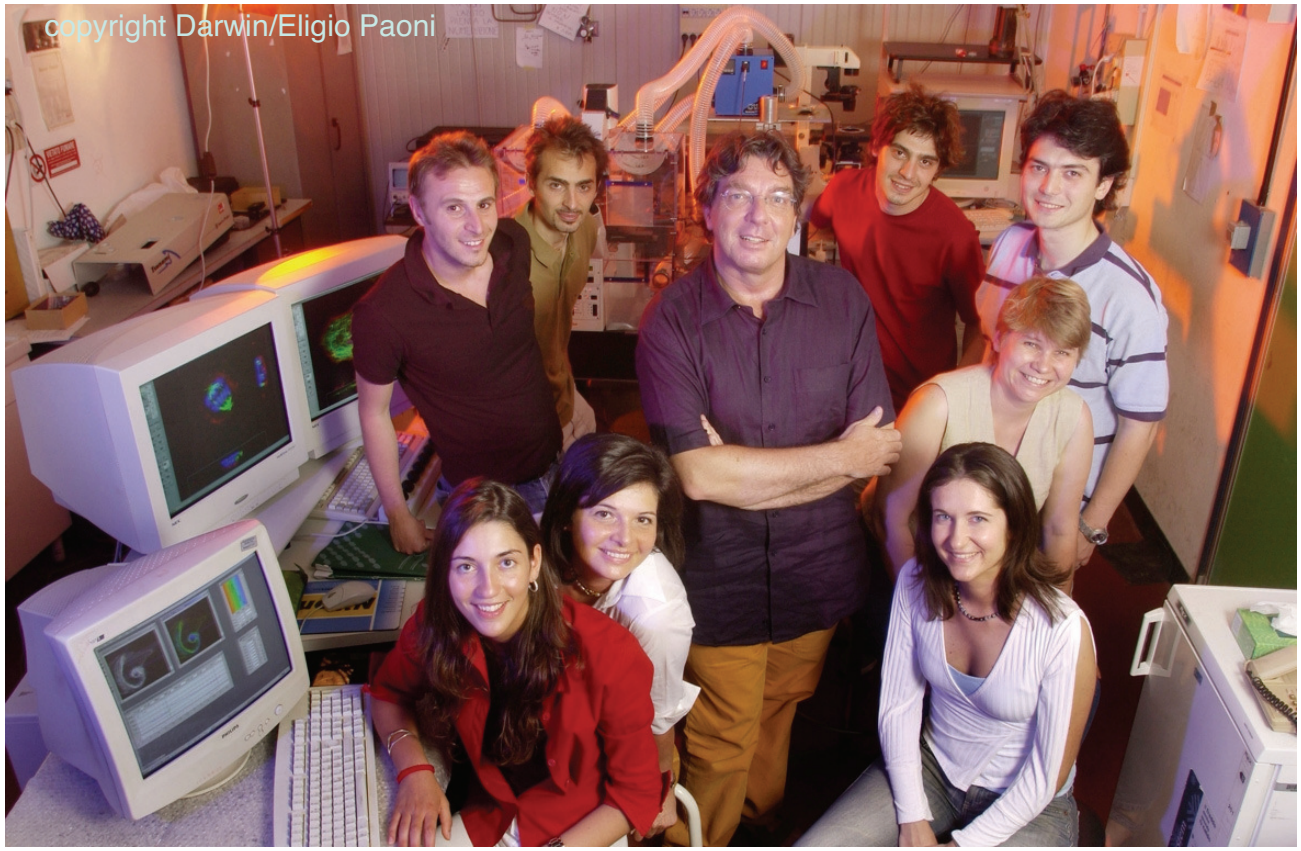

COMPAGNIA di San Paolo

difi

Università degli studi di Genova
Dipartimento di Fisica

IFOM

Festival della Scienza

LAMBS - MICROSCOBIO

lambs

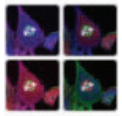

The Imaging Center of the IEO-IFOM Campus

Staff | Flow Cytometry | Confocal Microscopy | Fluorescence Microscopy | Live-Cell Video Microscopy | Microinjection | Image Analysis | Presentations Open Projects

Personnel

Mario Faretta
Facility coordinator and Scientist.
Wide Field and Confocal Fluorescence Microscopy, Time-lapse Microscopy, Flow Cytometry, Image Analysis, and SPR molecular interaction Analysis.
(Phone:0257489880)

IEO:

Simona Ronzoni
Flow Cytometry and Cell Sorting
(Phone:0257489880)

Ivan Muradore
Flow Cytometry
(Phone:0257489880)

Sara Barozzi
Fluorescence Microscopy and Cell Microinjection
(Phone:0257489880)

Francesca Refaldi
Flow Cytometry and Cell Sorting
(Phone:0257489880)

Dario Parazzoli
Fluorescence Confocal Microscopy and Image Analysis
(Phone:0257489880)

Search:

Enter search term

Search

IFOM:

Emanuela Frittoli
Fluorescence Microscopy and Cell Microinjection
(Phone:02574303324)

Massimiliano "Brutus" Garrè
Fluorescence wide field, Confocal and Time-lapse Microscopy
(Phone:02574303225)

Pietro Transidico
Fluorescence Confocal Microscopy and Image Analysis
(Phone:02574303225/258)

IFOM - IEO

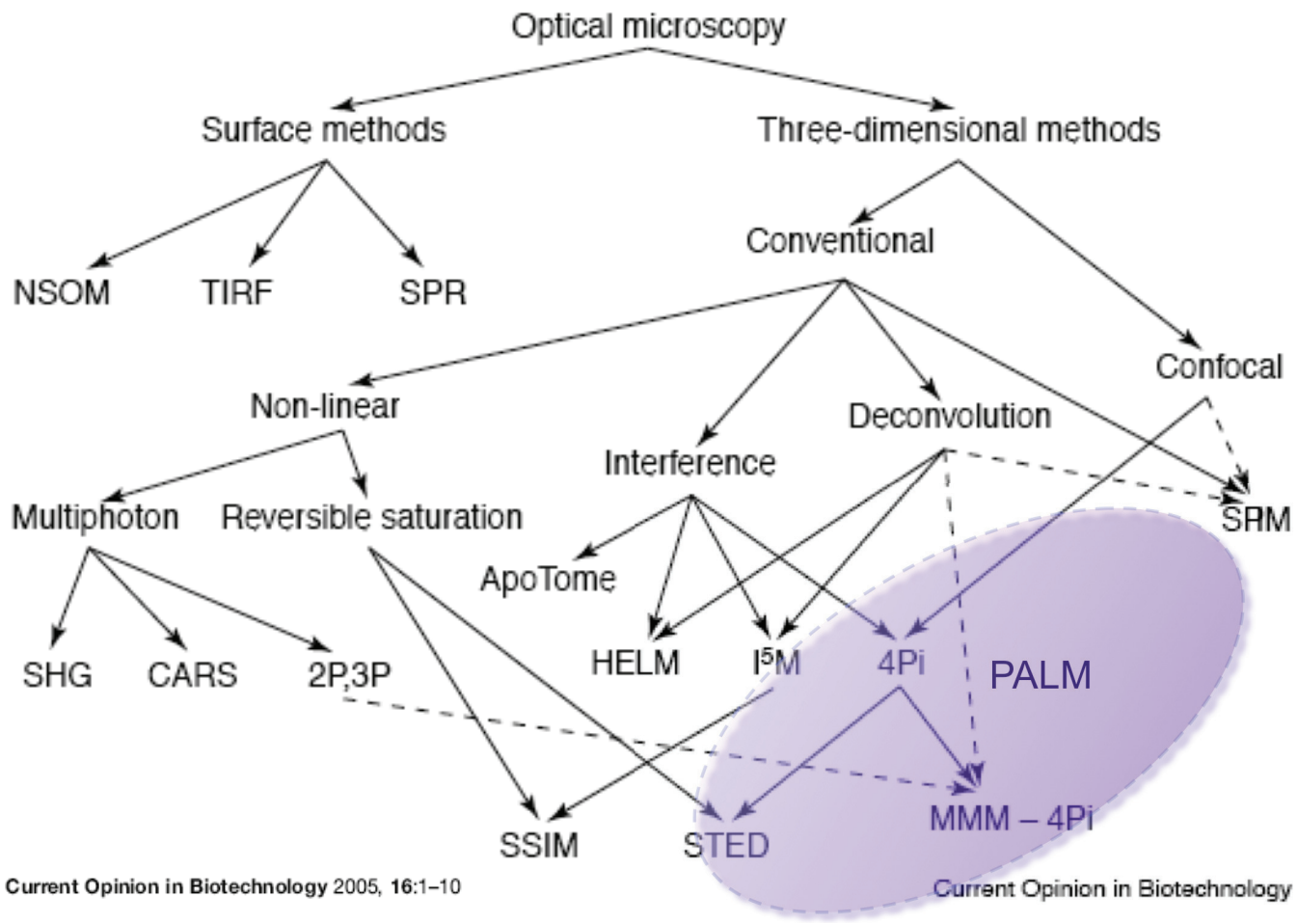

THE OPTICAL MICROSCOPY SCENARIO

HUMAN EYE 100 000 nm

OPTICAL MICROSCOPE 200 nm

ELECTRON MICROSCOPE 0.4 nm
3 nm

SCANNING PROBE MICROSCOPE 0.1-10 nm

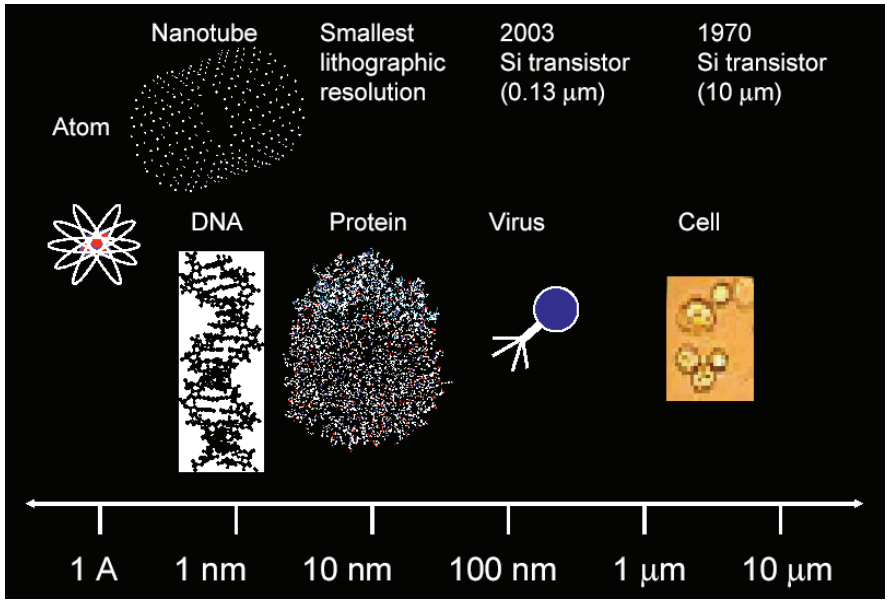

RESOLUTION OBSESSION

Slide credit: Stefan W. Hell, Max Planck Institute for Biophysical Chemistry, Department of NanoBiophotonics Göttingen

RESOLUTION OBSESSION

Journal of the
OPTICAL SOCIETY
of AMERICA

VOLUME 56, NUMBER 11 NOVEMBER 1966

Optical Systems with Resolving Powers Exceeding the Classical Limit*

W. LUKOSZ†
Institut A für Physik, Technische Hochschule, 33 Braunschweig, Germany
(Received 27 April 1966)

A new theorem on the ultimate limit of performance of optical systems is established: Not the bandwidth of the transferred spatial frequencies but only the number of degrees of freedom of the optical message transmitted by a given optical system is invariant. It is therefore possible (a) to extend the bandwidth by reducing the object area, (b) to extend the bandwidth in the x direction while proportionally reducing it in the y direction, so that the two-dimensional bandwidth is constant, and (c) to double the bandwidth when transmitting information about one state of polarization only.

To achieve this, the optical systems are modified by inserting two suitable masks (generally gratings) into optically conjugate planes of object and image space. The transfer and spread function of the modified systems are calculated for the case of coherent illumination.

INDEX HEADINGS: Optical systems; Diffraction; Polarization; Resolving power; Coherence.

Toraldo di Francia, G. Supergain antennas and optical resolving power. *Nuovo Cimento Suppl.* **9**, 426–435 (1952).

G. Toraldo di Francia, Rev. Opt. 28, 597 (1949).

RESOLUTION OBSESSION

(credit: EMILIO SEGRE' archive)

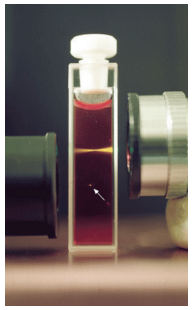

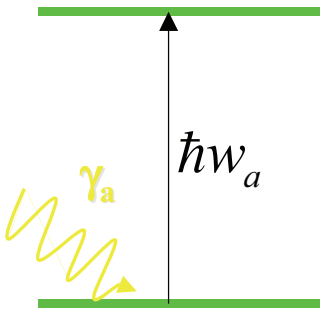

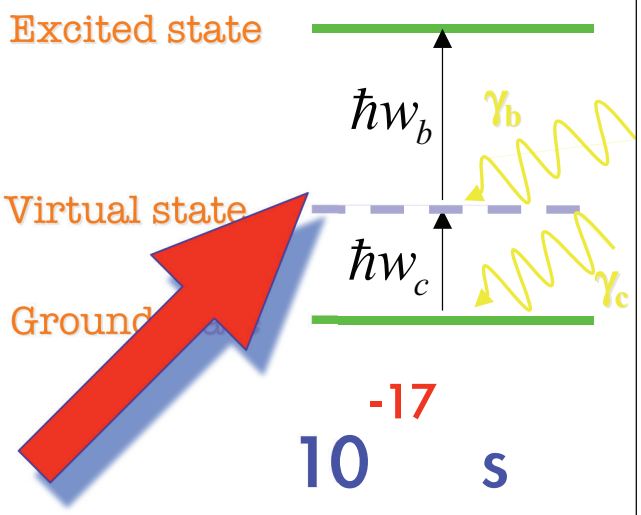

SIMULTANEOUSLY!

10^{-17} s

Maria Göppert-Mayer predicted that an atom or a molecule could interact with two photons simultaneously by absorbing them in the very same quantum event.

TWO-PHOTON EXCITATION

PHOTOACTIVATABLE - PROTEIN

Patterson GH, Lippincott-Schwarz J. (2002) Science 297:1873-1877.

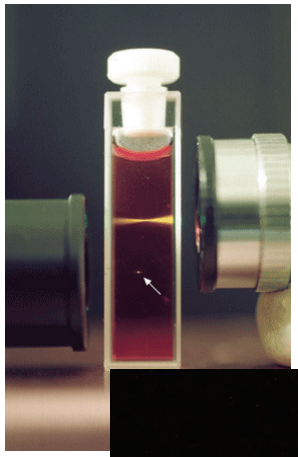

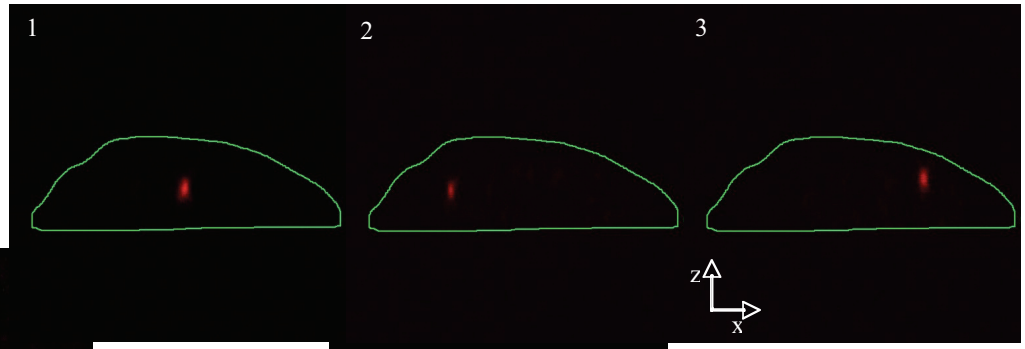

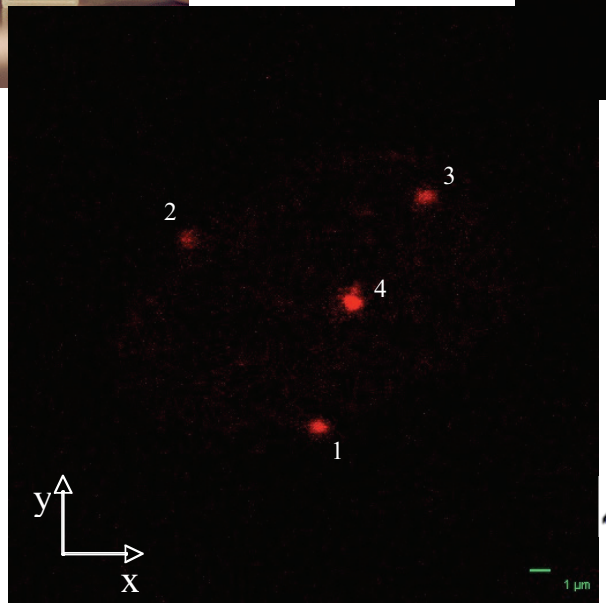

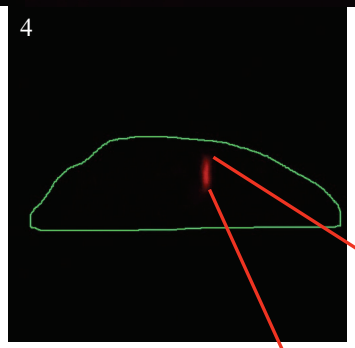

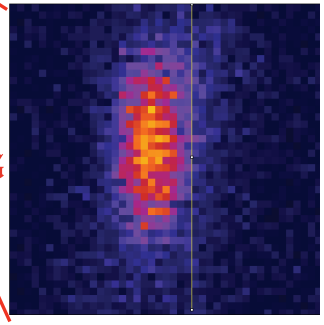

4D (X-Y-Z-T) SWITCHING

Schneider M., Barozzi S., Testa I., Faretta M., Diaspro A. Biophys. J., .89(2), 1346--1352 (2005).

Ilaria Testa, Dario Parazzoli, Sara Barozzi, Massimiliano Garrè, Mario Faretta, Alberto Diaspro , 2007 JBO

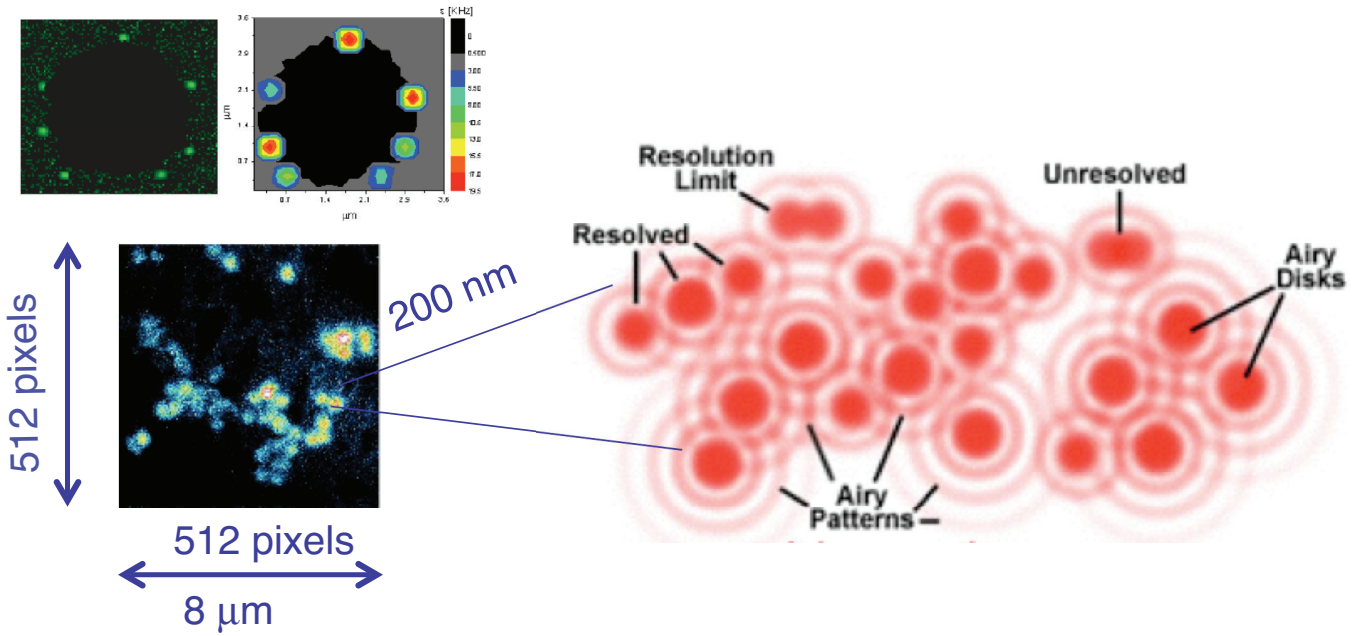

Single molecule structure is still not resolved

Chirico, G., Cannone, F., Beretta, S., Baldini, G., **Diaspro, A.**, Micr. Res. Tech., 55:359-364 (2002)
Chirico G., Cannone F., Baldini G., and **Diaspro A.** Biophysical J., 84 (2003).
Chirico G., Cannone F., and **Diaspro A.**, J.Phys.D,36 (2003).

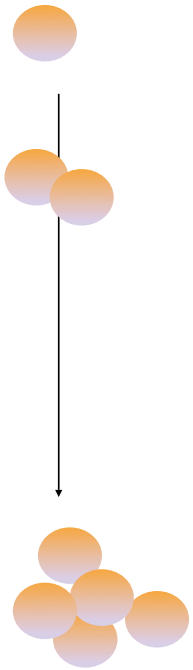

Intensity χ

Intensity 2χ

Intensity $N\chi$

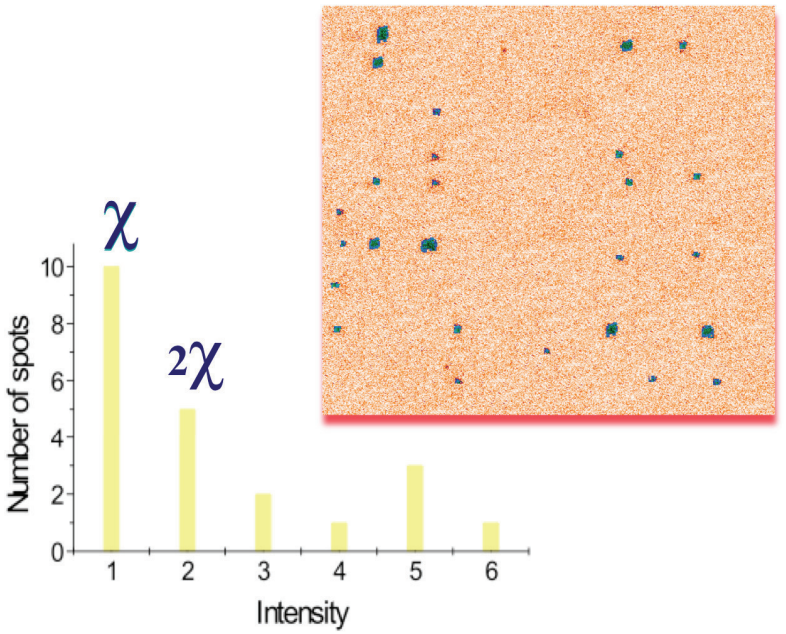

N = number of molecules

Micr. Res. Tech. (2002) 55:359-4

SINGLE MOLECULE IMAGING

Fluorescein c=1µM @ 8mW

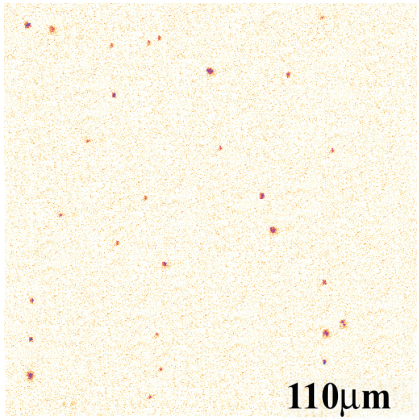

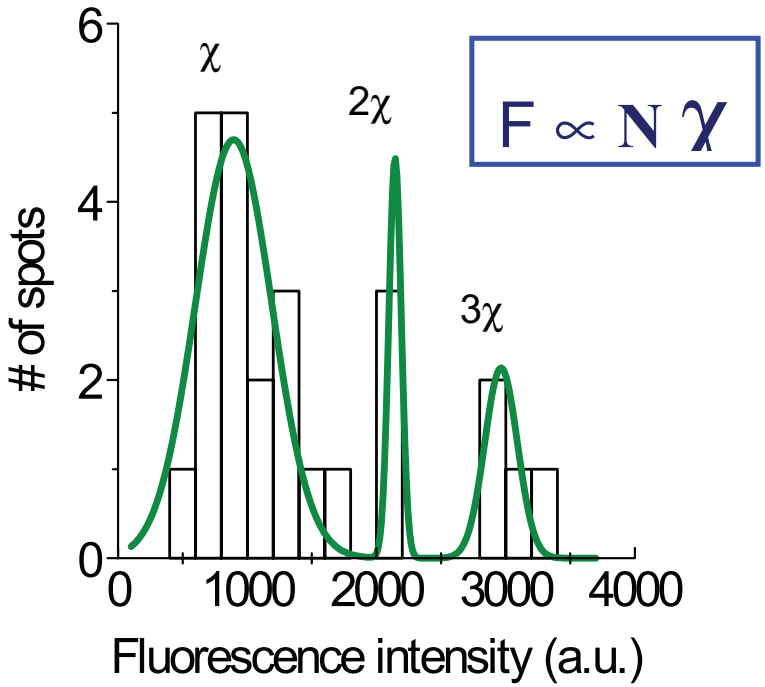

Micr. Res. Tech. (2002) 55:359-4

Single Molecule

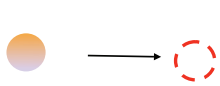

Aggregates

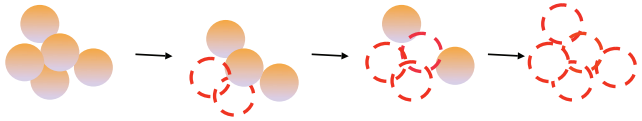

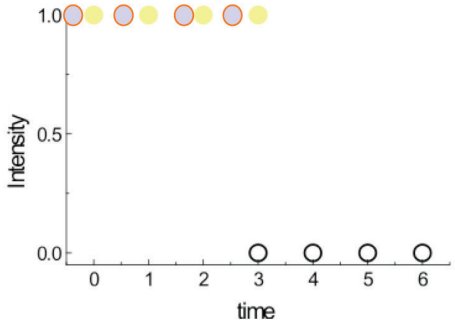

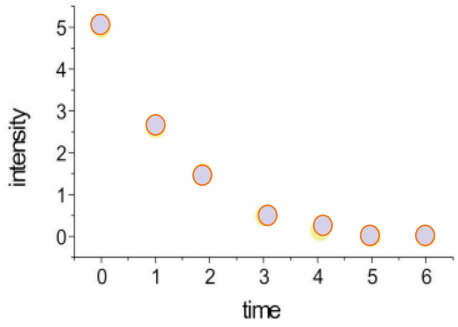

Micr. Res. Tech. (2002) 55:359-4

SINGLE MOLECULE IMAGING

Fluorescence Polarization

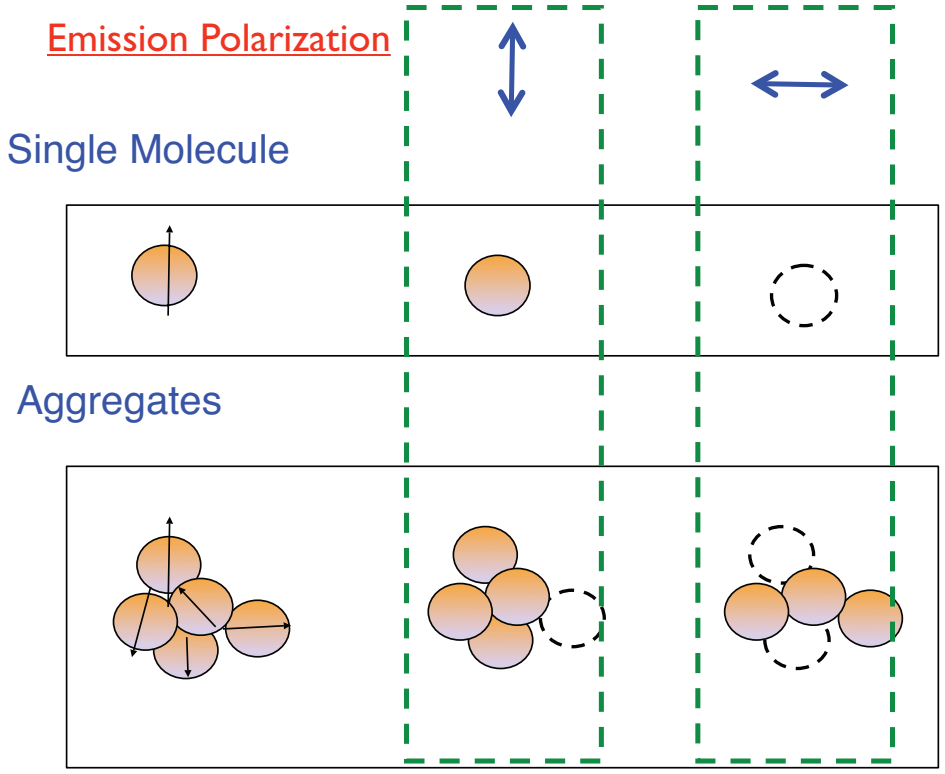

J Biomed Opt. (2003) 8(3):391-5

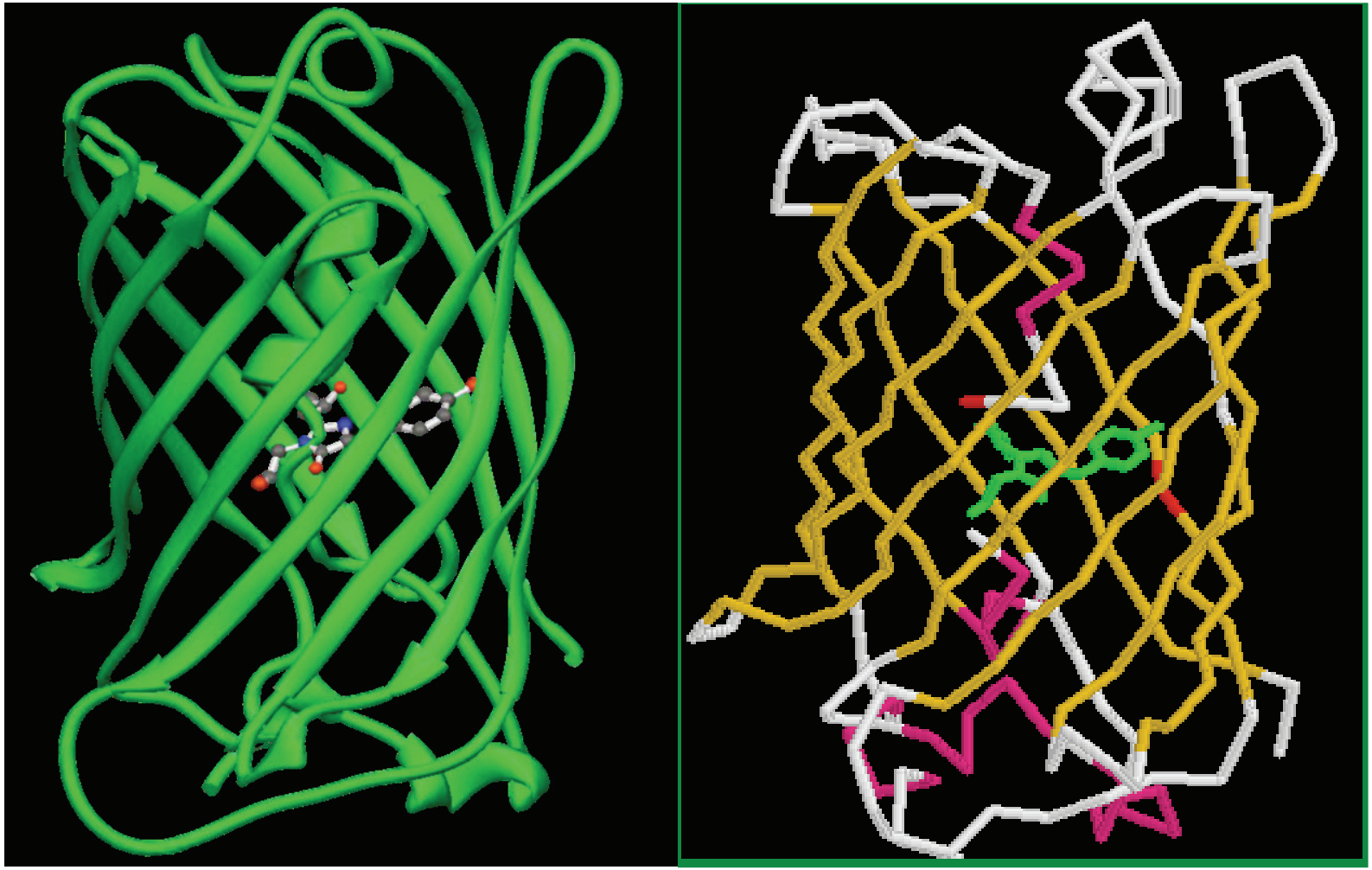

GFP PHOTOPHYSICS

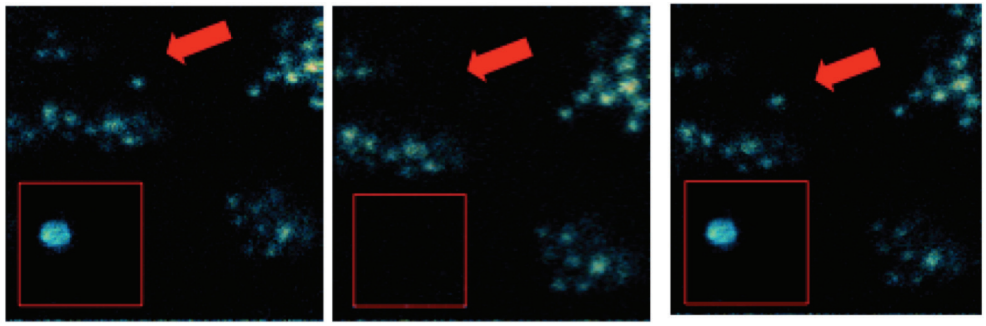

TPE @ 785 nm TPE @ 720 nm TPE @ 785 nm

Cinelli RA, Ferrari A, Pellegrini V, Tyagi M, Giacca M, Beltram F.,Photochem Photobiol. 2000 71(6):771-6.

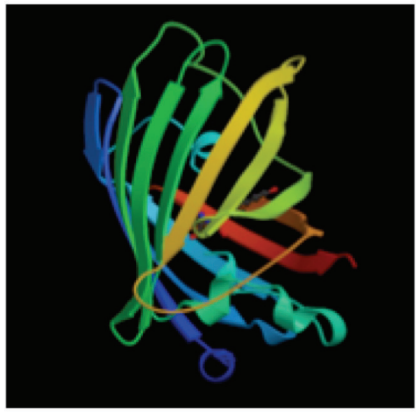

E^2GFP in silica GEL, maximum excitation within 700-800 nm range @ 785; after imaging photobleaching @ 785; photocycling @ 720 nm - no photorecovery @ 710/730 -; final imaging @ 785.

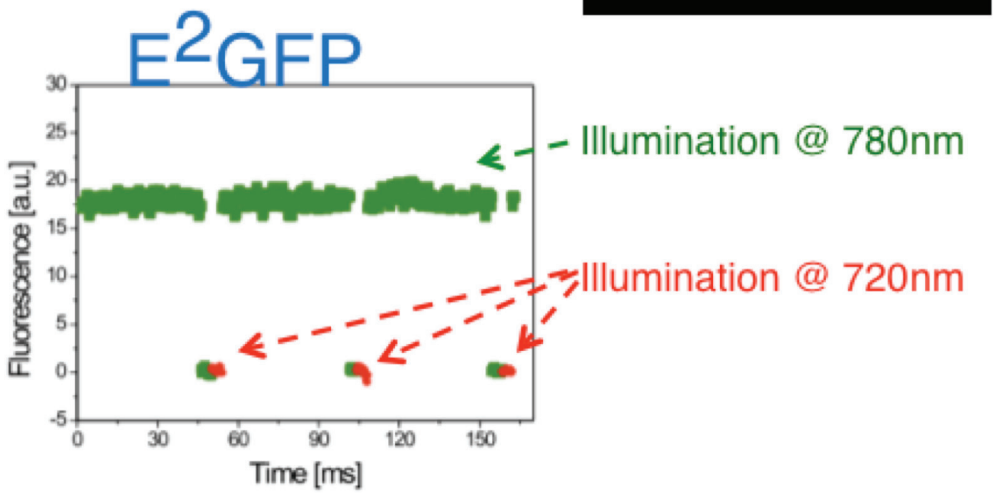

Phys Rev E Stat Nonlin Soft Matter Phys. 2004 Sep;70(3 Pt 1):030901

GFP PHOTOPHYSICS

E^2GFP

Two Photon Switching Protein

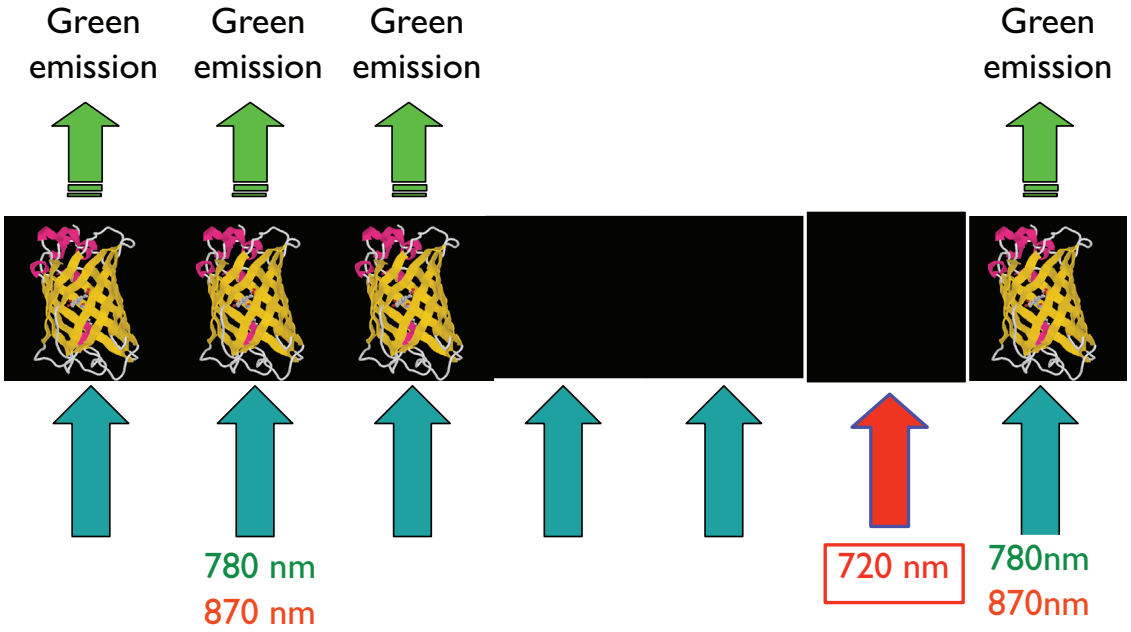

SWITCHABLE - GFP - SINGLE MOLECULE

PHYS REV E STAT NONLIN SOFT MATTER PHYS. 2004 SEP;70(3 PT 1):030901

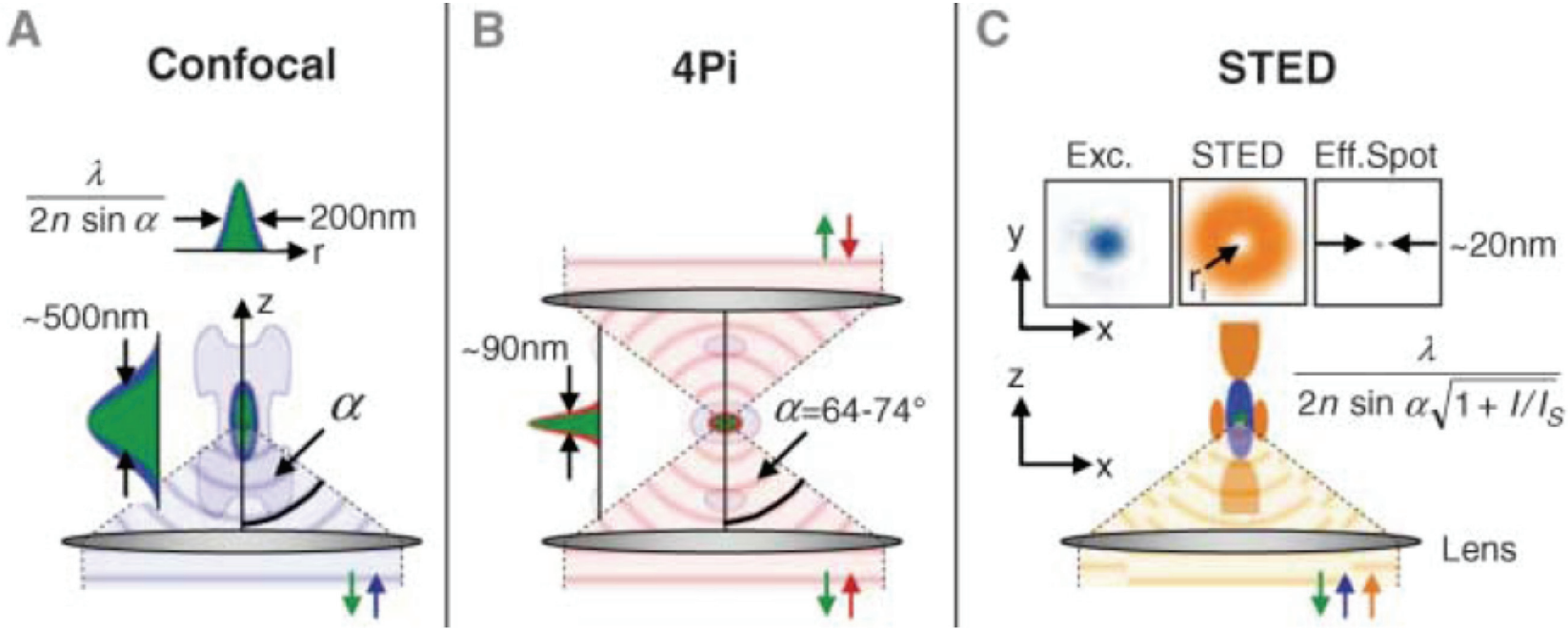

S.W. Hell, et al. **Far-Field Optical Nanoscopy,** Science **316**, 1153 (2007)

FROM MICROSCOPY TO NANOSCOPY

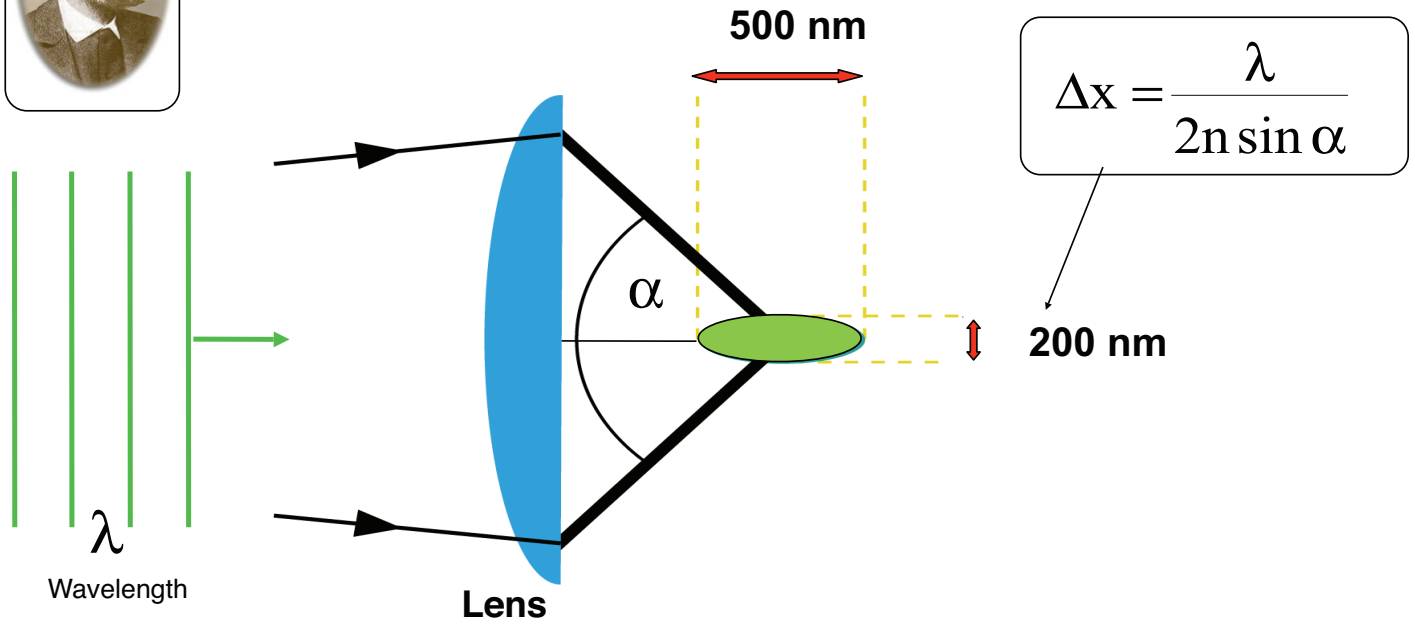

ABBE, E (1873) ARCHIVE F. MIKROSKOP.ANAT. 9, 413-420

Slide credit: Stefan W. Hell, Max Planck Institute for Biophysical Chemistry, Department of NanoBiophotonics Göttingen

OPTICAL RESOLUTION

4Pi- Microscopy:

Coherent illumination and/or fluorescence detection

70 - 140 nm

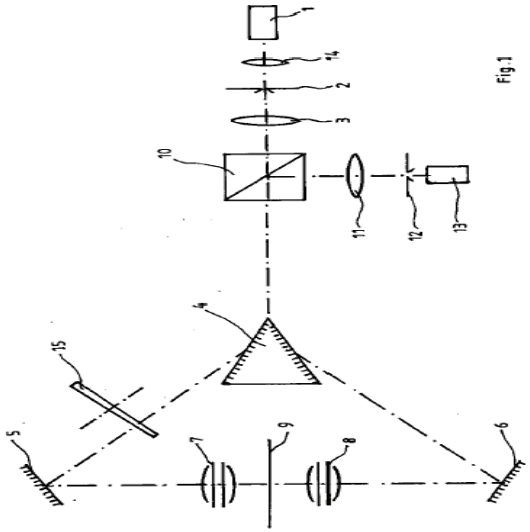

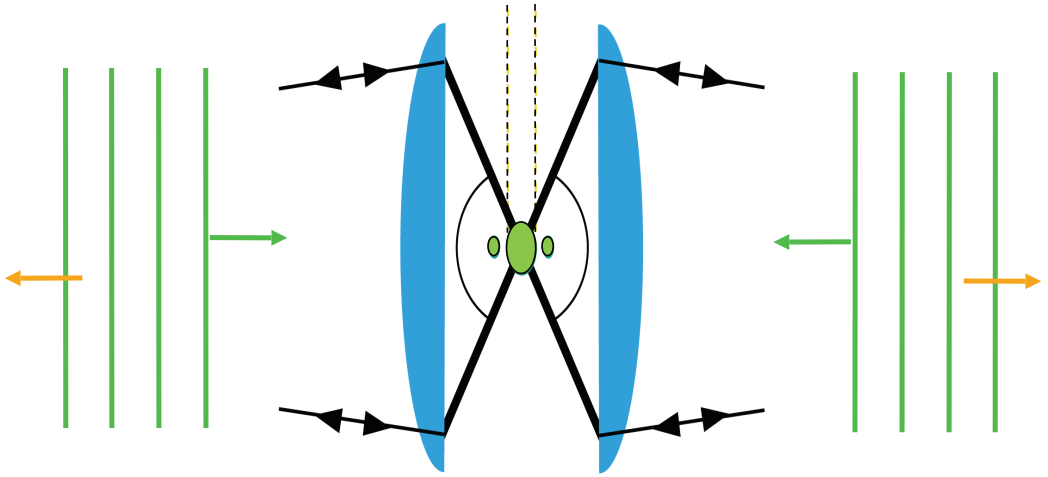

$$\vec{E}^{4Pi}(r,z,\varphi) = \vec{E}_1(r,z,\varphi) + \vec{E}_2(r,-z,\varphi)$$

4Pi microscopy coherently illuminates the sample through two opposing lenses. Constructive interference of the counterpropagating spherical wavefronts narrows the main focal maximum of the excitation light in the z-direction, and this forms the basis for a 3- to 7-fold improved axial resolution.

S.W. Hell (1990), Europ. Patent OS 0491289.
S.W. Hell, et al. (1992), Opt. Commun. **93**, 277.
M. Schrader, et al. (1998), Biophys. J. **75**, 1659.
H. Gugel, et al. (2004), Biophys. J. **87**, 4146.

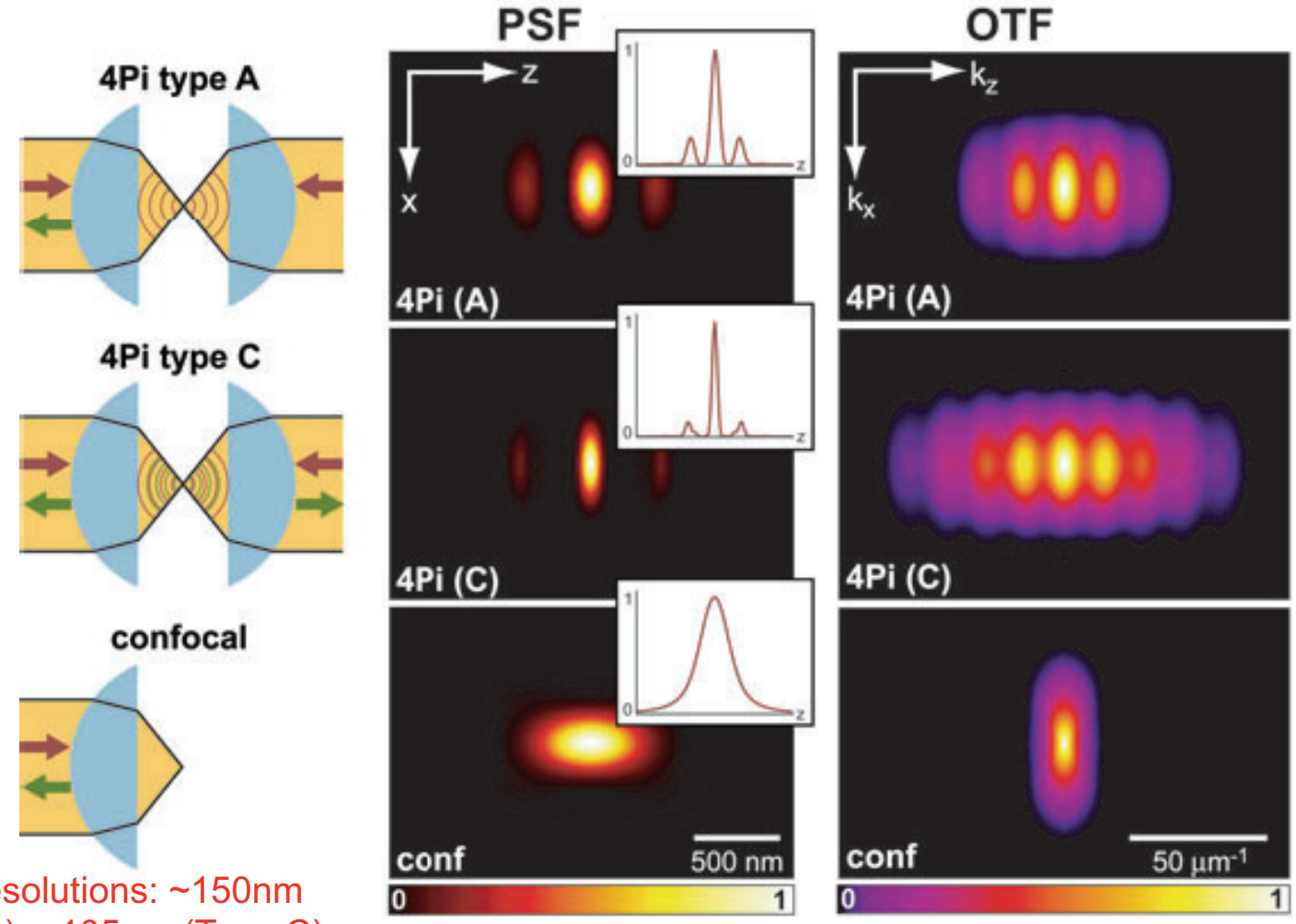

Axial resolutions: ~150nm (Type A), ~105nm (Type C)

theoretical z-response of a thin film

2-photon / 840 nm
1.35NA oil immersion

confocal

4 Pi (A)

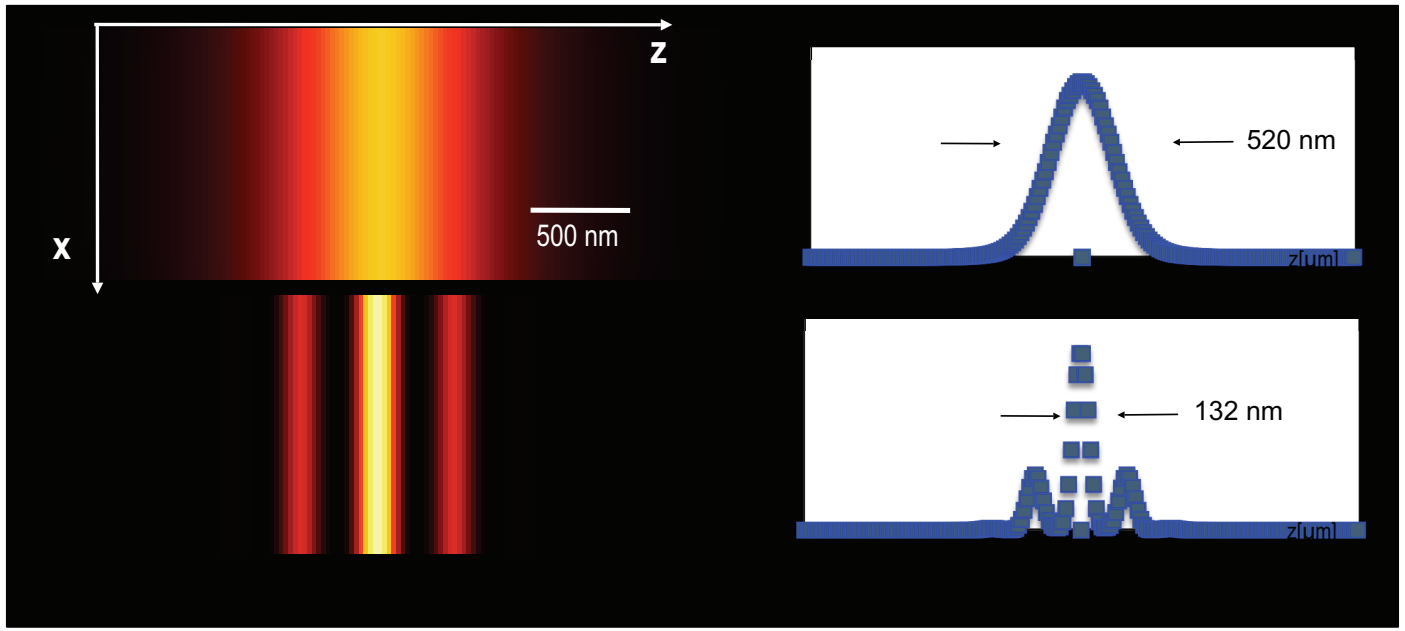

z[µm]

experimental z-response of a fluorescent layer

2-photon / 840 nm
1.4 NA oil immersion

confocal

4 Pi

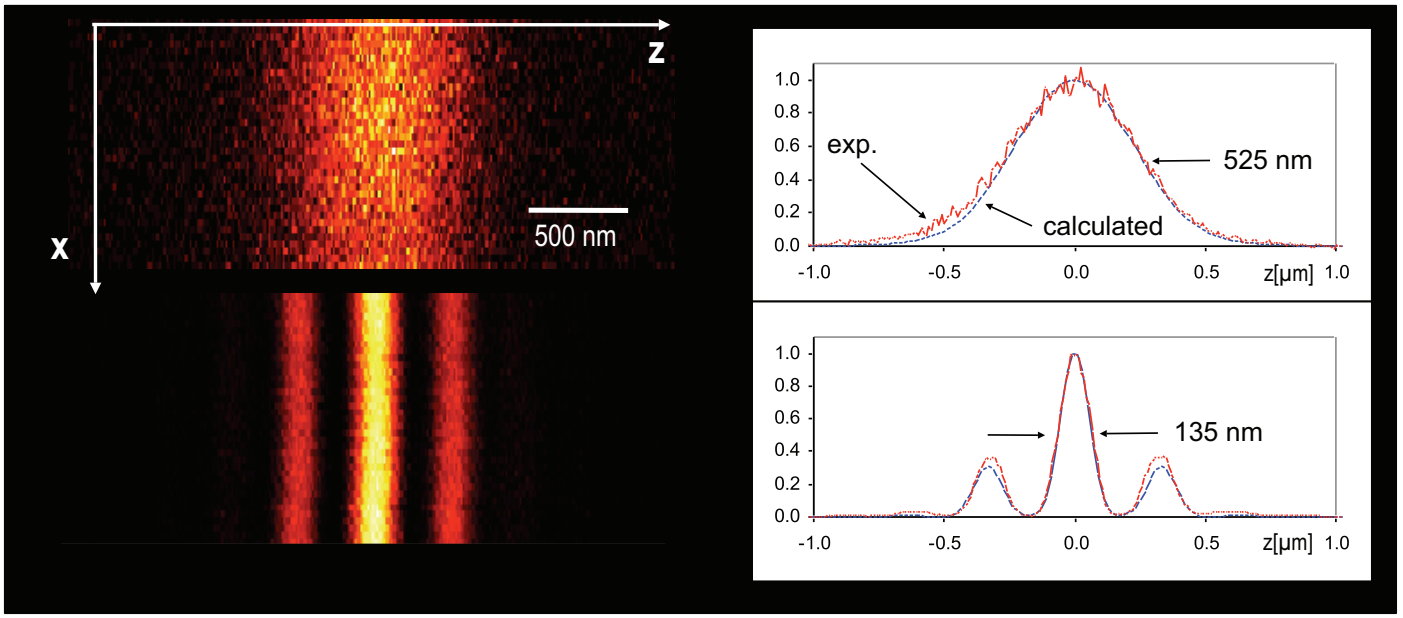

Vicidomini, G., Schneider, M., Bainchini, P., Krol, S., Szellas, T. & Diaspro, A. (2007) **J. Microscopy**, vol. 225, pp. 88-95.

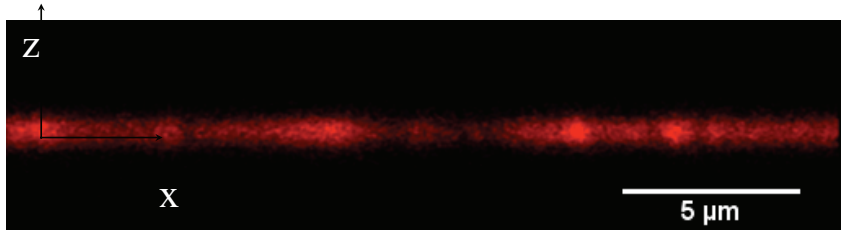

Confocal Laser Scanning Microscopy (CLSM)

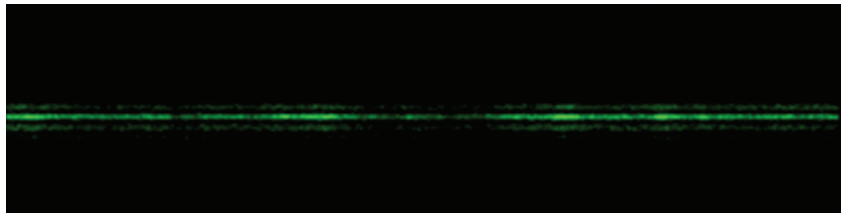

Two-Photon Excitation 4Pi Microscope (TPE4Pi)

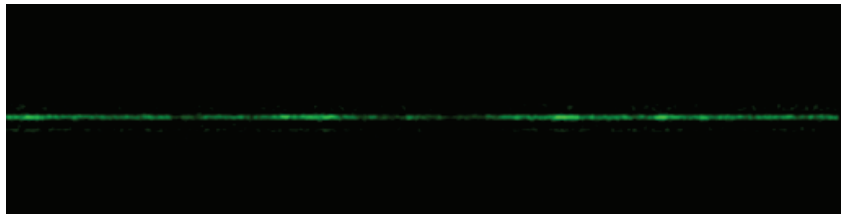

TPE4Pi after deconvolution

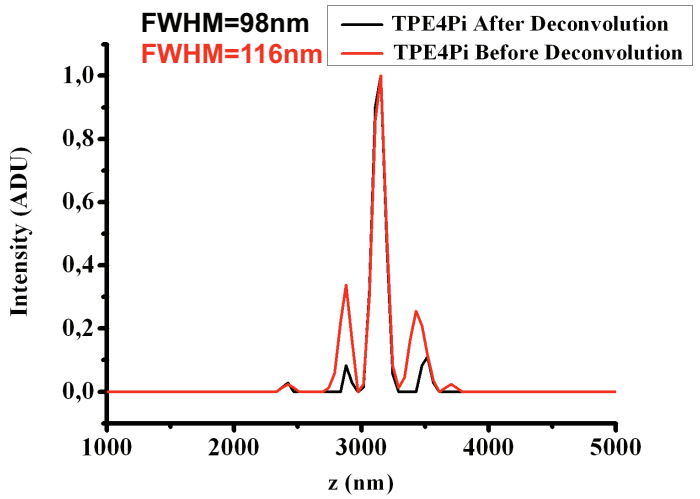

4Pi Microscopy: geometry of sample

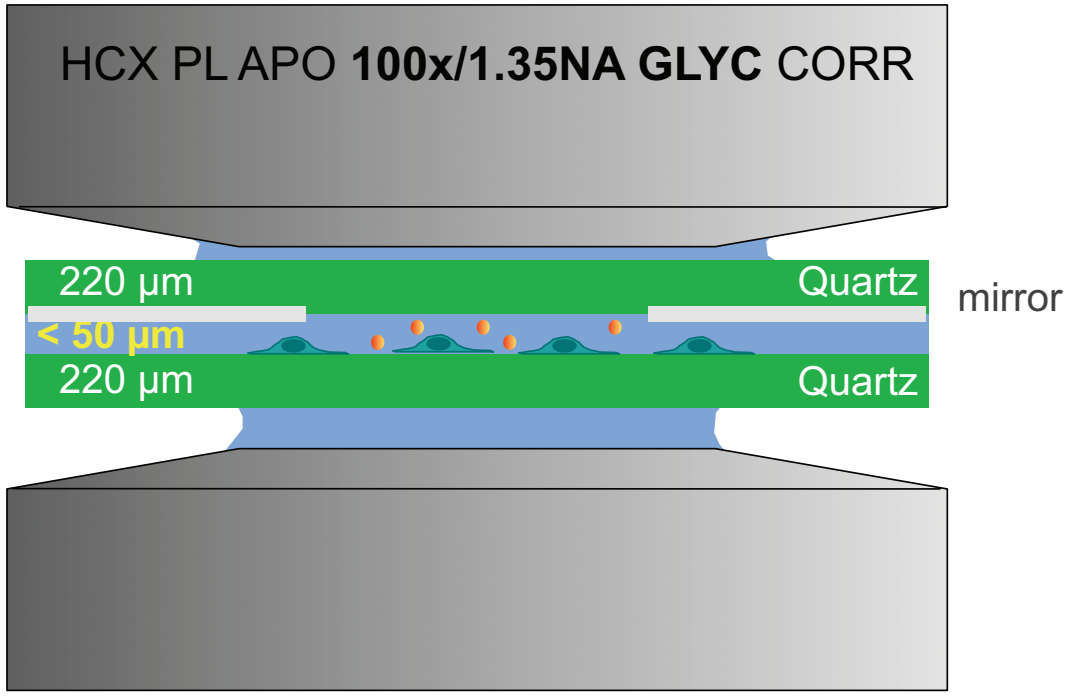

4Pi Microscopy: sample preparation

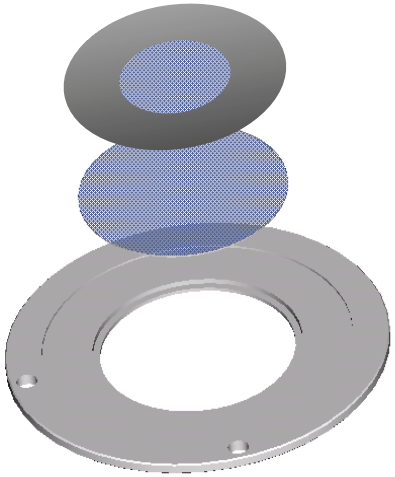

- Thickness of the sample < 50µm (distance between the 2 coverslips < 100 µm)
- Coverslips on both sides (Quartz coverslips for best optical performance in combination with glycerol objectives)
- Embedding medium with same refractive index as immersion medium (75% - 85% Glycerol)
- 1 mirrored coverglas for 4Pi adjustment
- 100nm beads added to the sample for quality check

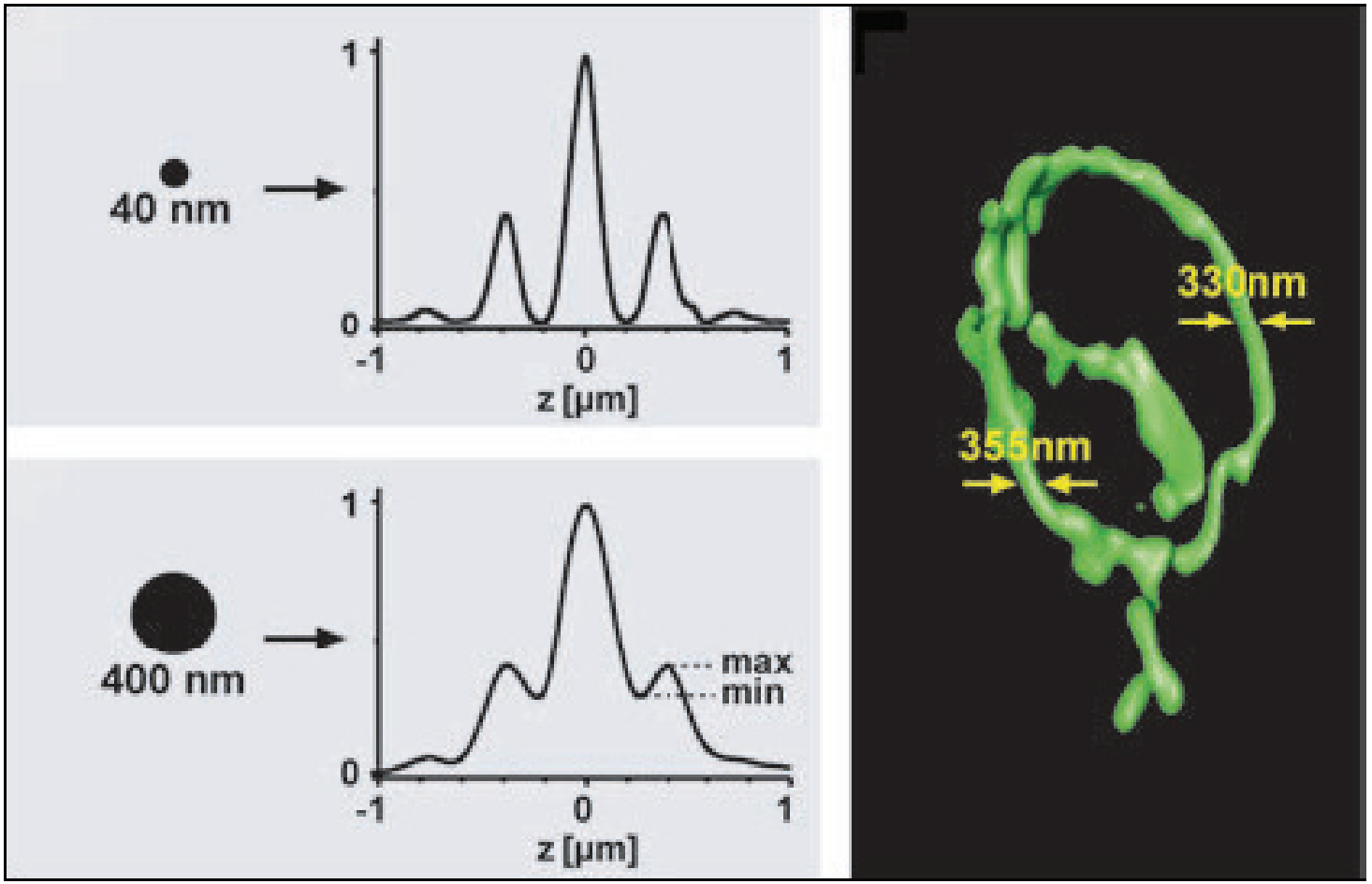

This figure illustrates the determination of the diameter of mitochondria in a yeast cell, following calibration.

NATURE BIOTECHNOLOGY VOLUME 21 NUMBER 11 NOVEMBER 2003

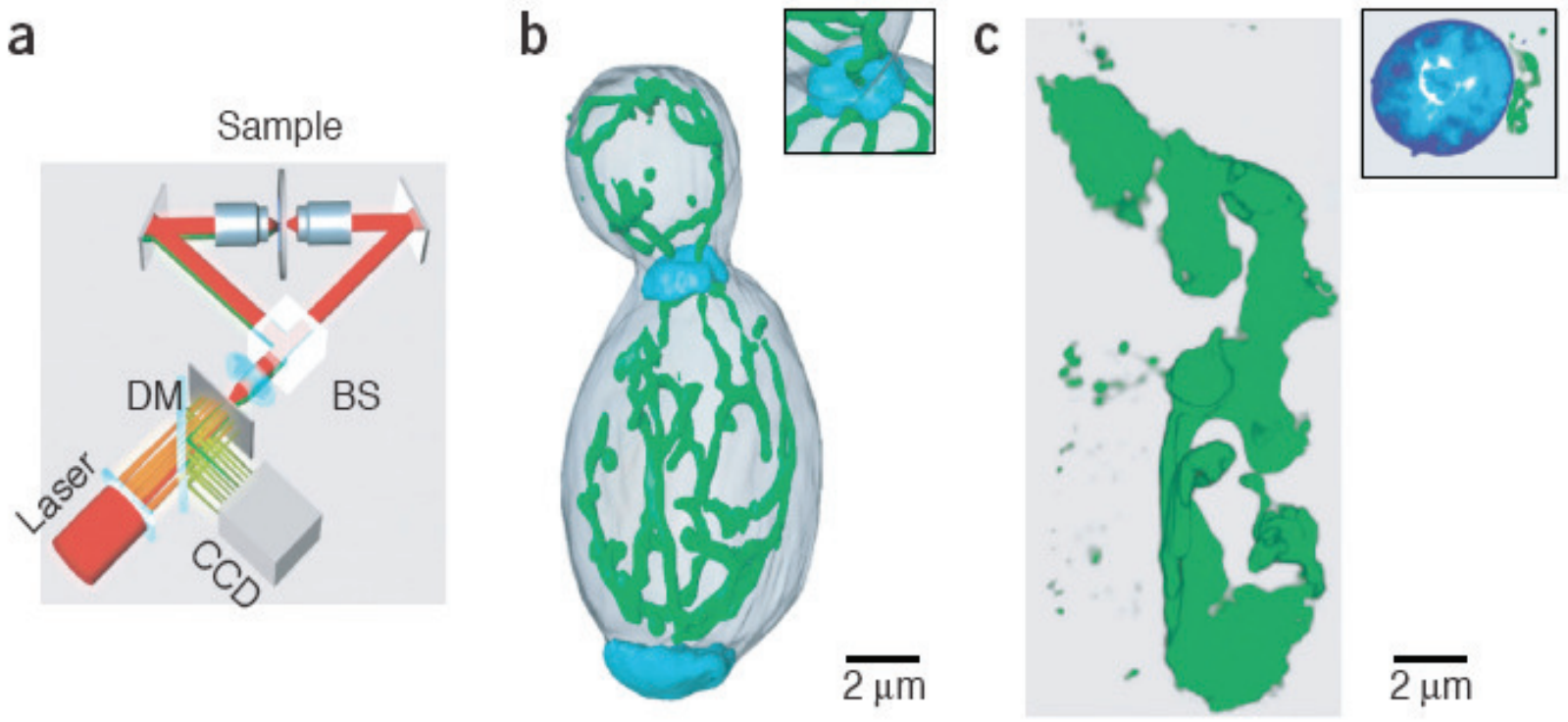

GFP labeled Mithocondria (b) and Golgi (c)

Egner, A., Jakobs, S. & Hell, S.W. Fast 100-nm resolution 3D-microscope reveals structural plasticity of mitochondria in live yeast. *Proc. Natl. Acad. Sci. USA* **99**, 3370–3375 (2002).

. Egner, A., Goroshkov, A., Verrier, S., Söling, H.-D. & Hell, S.W. Golgi apparatus of live mammalian cell at 100 nm resolution. *J. Struct. Biol.* in the press (2003).

Stimulated Emission Depletion (STED) Fluorescence Microscopy

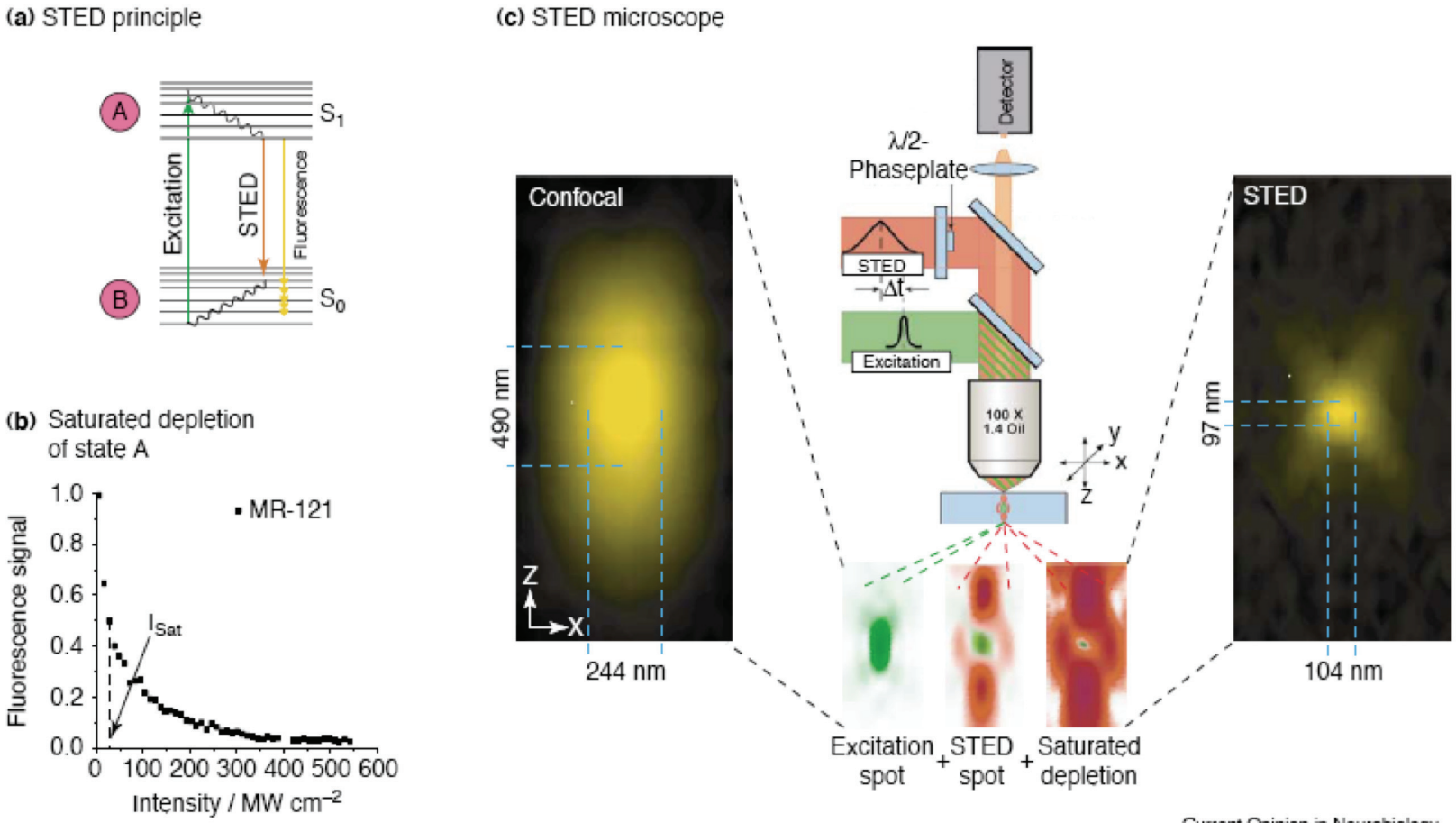

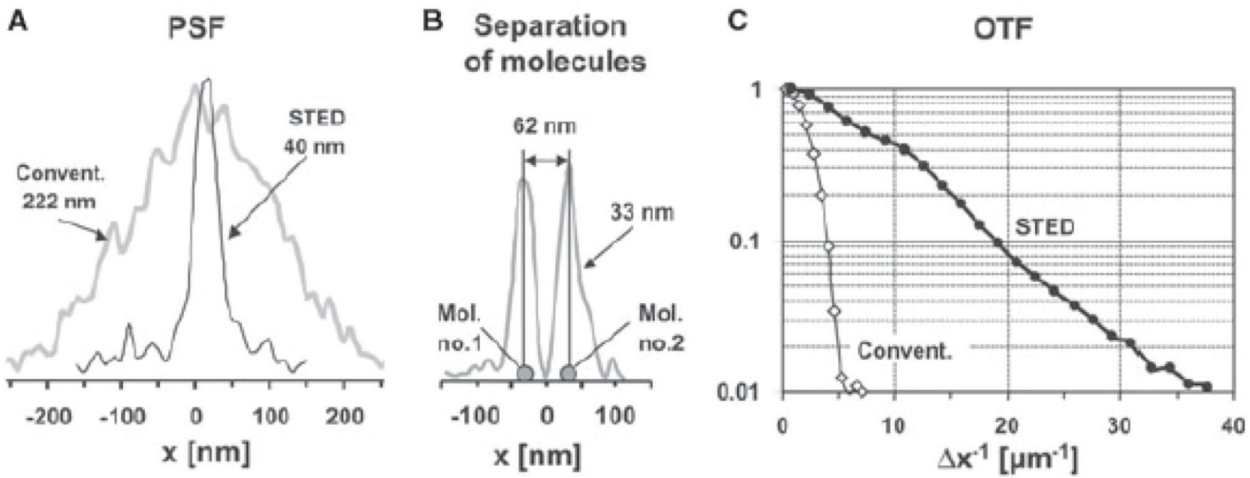

Quantifying lateral resolution in STED microscopy through imaging of point-like objects. (A) The effective point spread function (PSF) of a conventional microscope and a (laser-diode) STED microscope, determined on single dye molecules (JA 26). (B) Molecules spaced apart far below the diffraction limit could be clearly separated in STED microscopy (slightly augmented by deconvolution). (C) For STED microscopy the gain in transmitted bandwidth of the optical transfer function (OTF) is more than 5-fold, compared with conventional microscopy. Objective lens, NA = 1.4 (oil); wavelengths λ, 635 nm (excitation), 650 to 720 nm (fluorescence detection), 781 nm (STED).

Category	Name	Emission nm	STED nm	Manufacturer	Notes
Green dye*	Atto532	540–570	615	Atto-tec GmbH, Siegen, DE	Used for single-molecule studies
Yellow dye*	DY-510XL	560–630	625	Dyomics GmbH, Jena, DE	Immunofluorescence label
Red dye*	Atto647N	650–720	760	Atto-tec GmbH, Siegen, DE	Used for single-molecule studies
Far red dye	Pyridine 2	680–750	750–780	SigmaAldrich, St. Louis, MO	Membrane label
Infrared dye	Pyridine 4	710–800	780–800	SigmaAldrich, St. Louis, MO	Membrane label

STED Microscopy

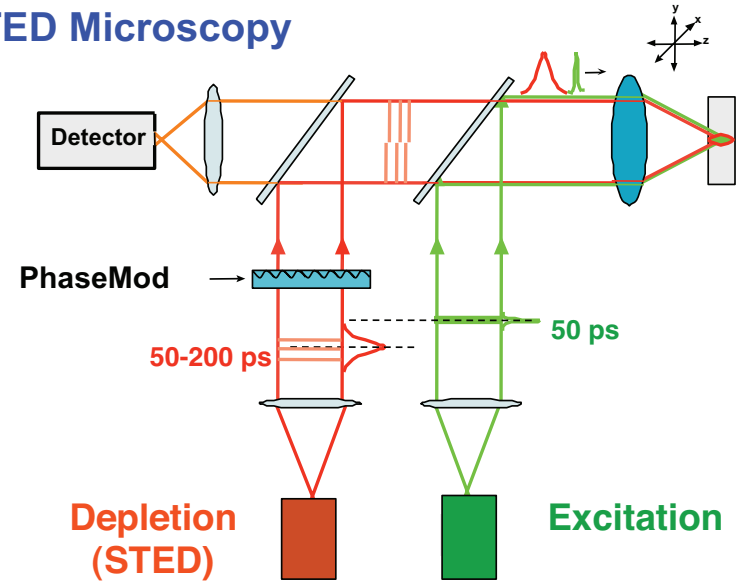

S.W. Hell & J. Wichmann (1994), *Opt. Lett.* **19**, 780.

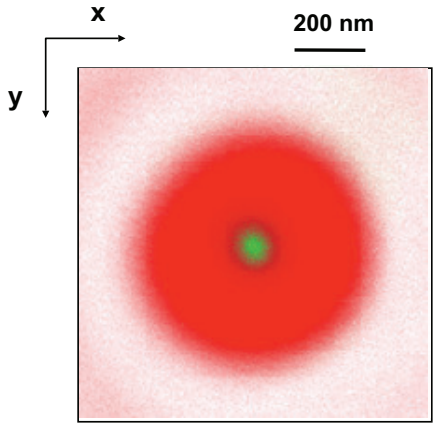

The stronger the STED beam the narrower the fluorescent spot!

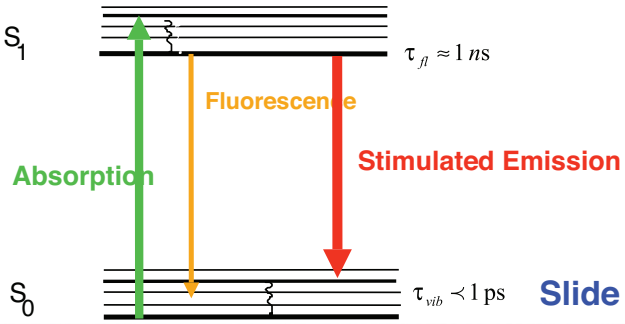

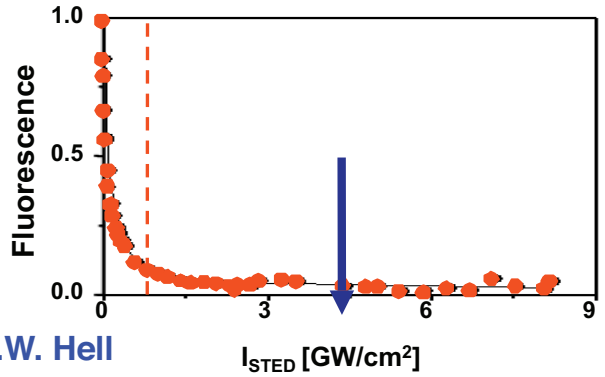

Slide credit: S.W. Hell

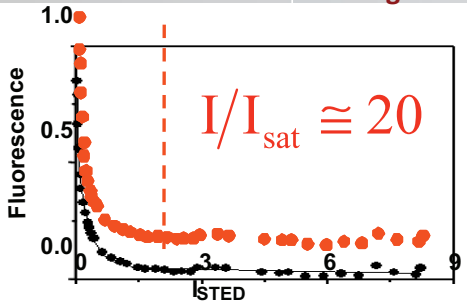

Focal spot ... probed with 1 molecule

λ_{STED}= 770 nm

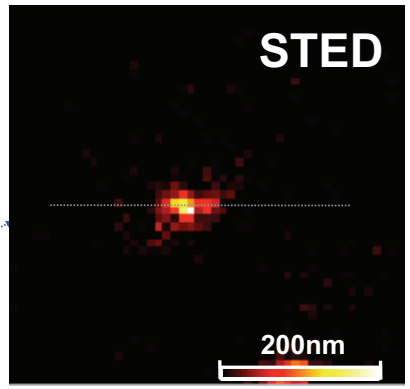

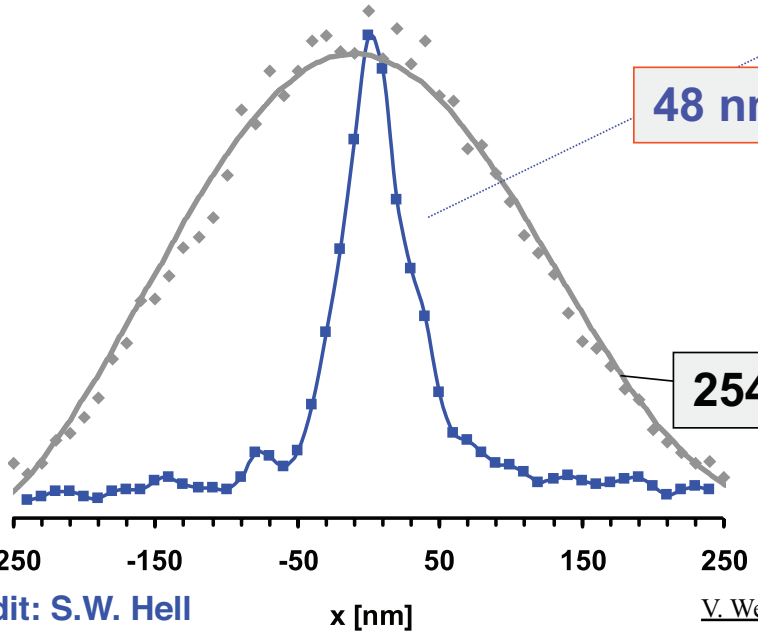

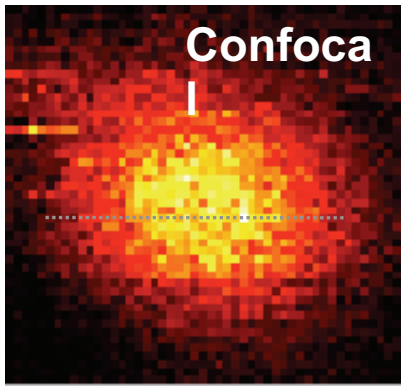

Slide credit: S.W. Hell

V. Westphal & S.W. Hell (2005), Phys. Rev. Lett. **94**, 143903.

Confocal

STED

40 nm beads (Molecular Probes)

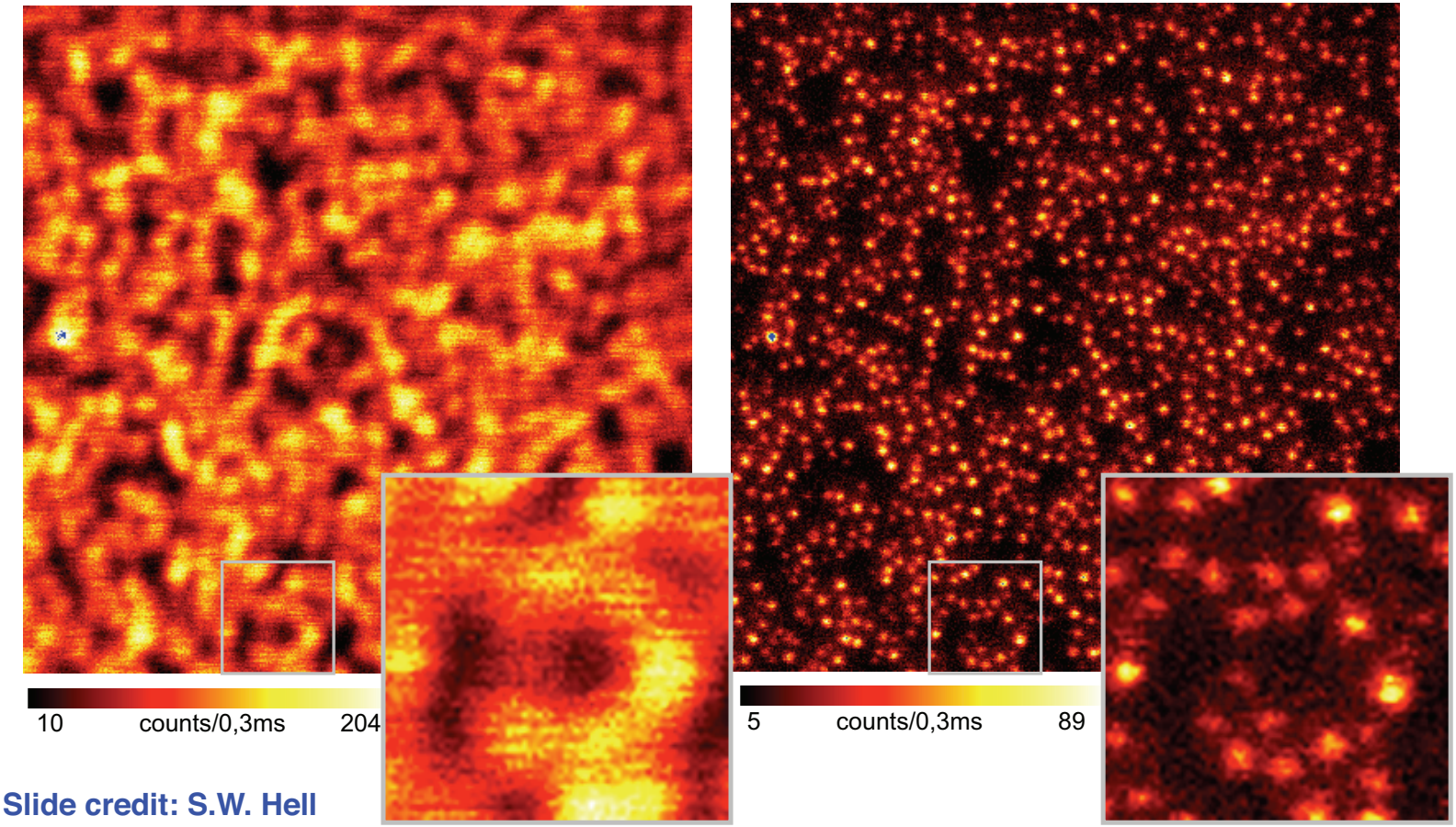

Slide credit: S.W. Hell

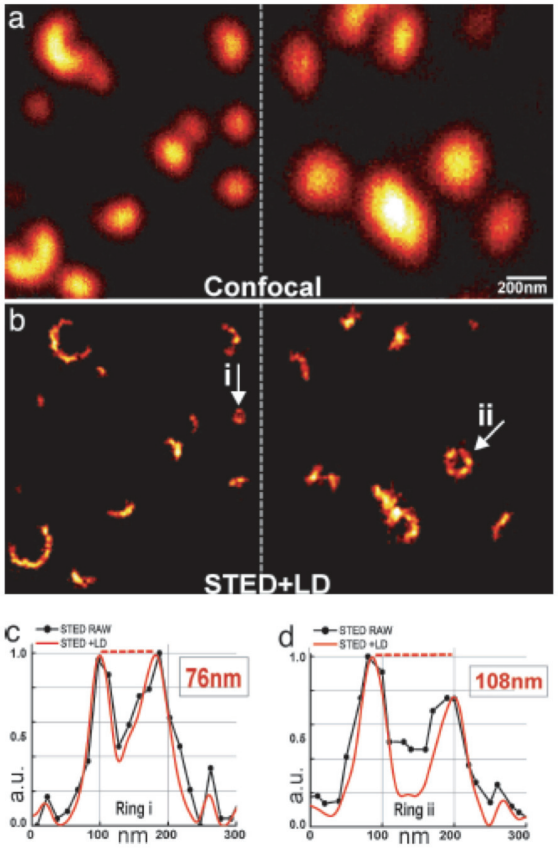

Fig. 4. Synaptophysin forms elaborate nanopatterns on endosomes. (*a*) Confocal reference. (*b*) STED microscopy plus a LD (see *Material and Methods*) revealing ring-like and C-shaped nanoarrangements. (*c* and *d*) Line profiles through rings, both of the LD (red line) and of the raw STED data (black, with pixels).

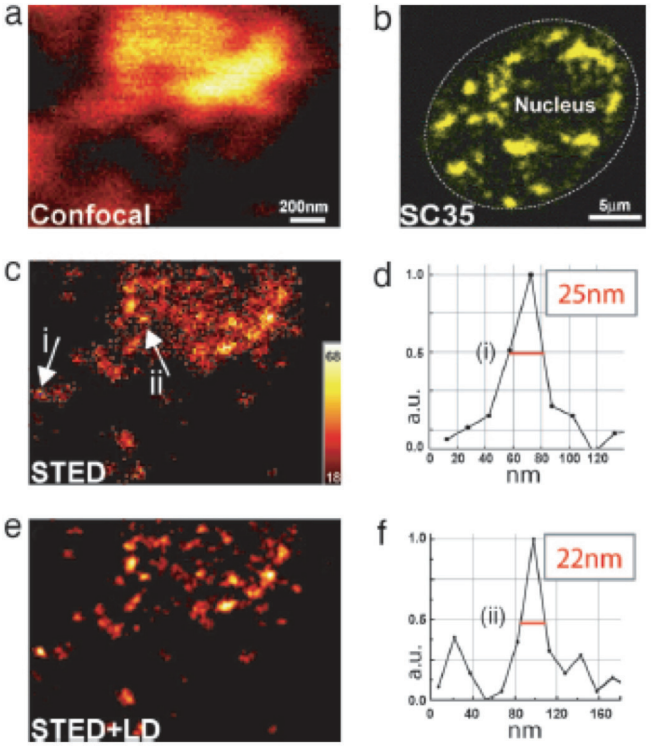

Fig. 5. Resolving the nanostructure of speckles of protein SC35 in intact mammalian cell nuclei. (*a*, *c*, and *e*) Confocal image of a speckle domain (*a*) with STED counterpart data, raw (*c*) and after LD (*e*). (*b*) Conventional overview image of speckles in nucleus. (*d* and *f*) Raw data profiles through speckle nanofeatures indicate a STED microscopy lateral resolution of ~20 nm in the nucleus.

PALM (photoactivated localization microscopy) is an optical method for imaging intracellular proteins at nanometer spatial resolution.

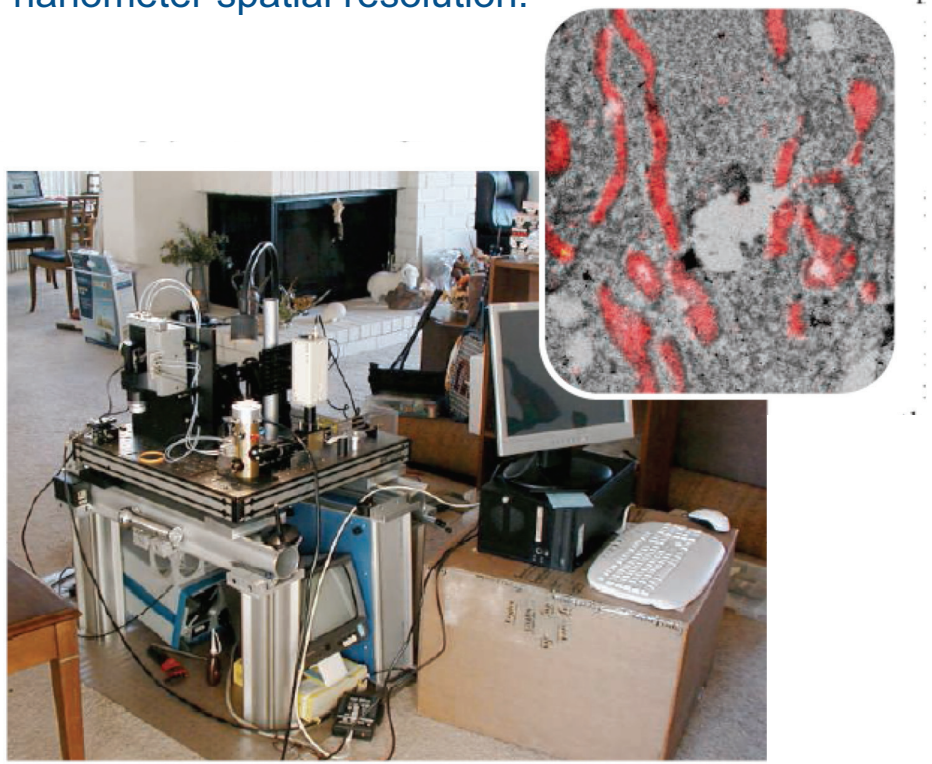

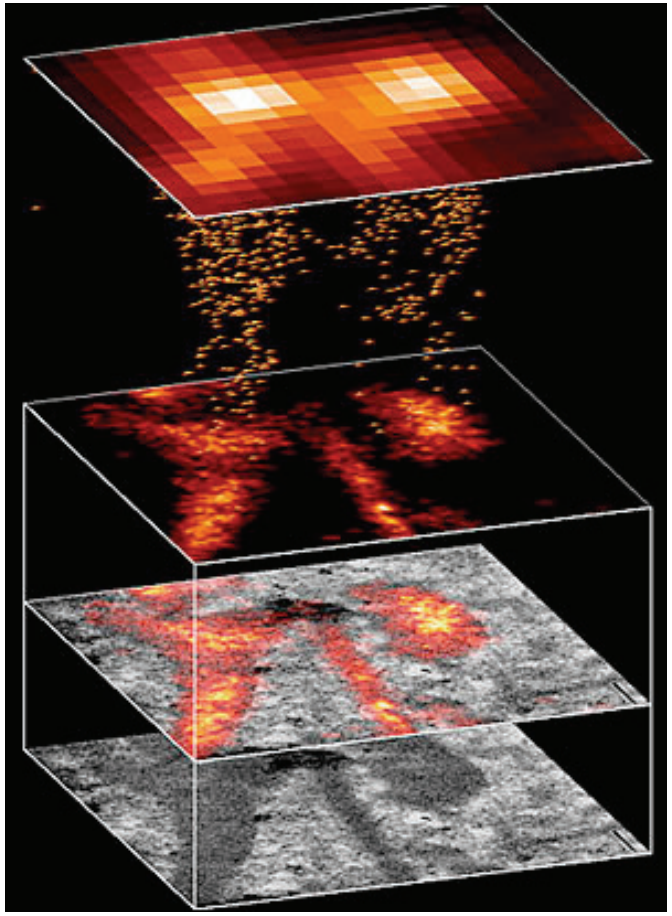

Betzig E, Patterson GH, Sougrat R, Lindwasser OW, Olenych S, Bonifacino JS, Davidson MW, Lippincott-Schwartz J, Hess H. Imaging intracellular fluorescent proteins at nanometer resolution. Science. 2006 Sep 15;313(5793):1642-5.

Numerous sparse subsets of photoactivatable fluorescent protein molecules are activated, localized (to approx.2 to 25 nanometers), and then bleached. The aggregate position information from all subsets is then assembled into a superresolution image.

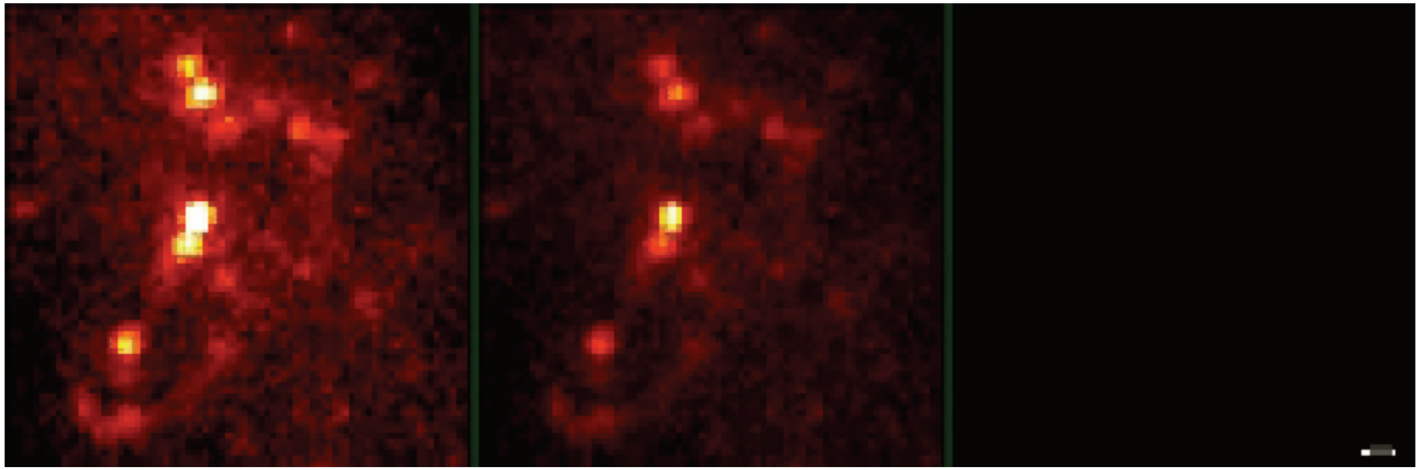

The performances are largely dictated by the photophysical characteristics of the PA-FPs.

This method has been used to image specific target proteins in thin sections of lysosomes and mitochondria; in fixed whole cells, we imaged vinculin at focal adhesions, actin within a lamellipodium, and the distribution of the retroviral protein Gag at the plasma membrane.

Betzig E, Patterson GH, Sougrat R, Lindwasser OW, Olenych S, Bonifacino JS, Davidson MW, Lippincott-Schwartz J, Hess H. Imaging intracellular fluorescent proteins at nanometer resolution. Science. 2006 Sep 15;313(5793):1642-5.

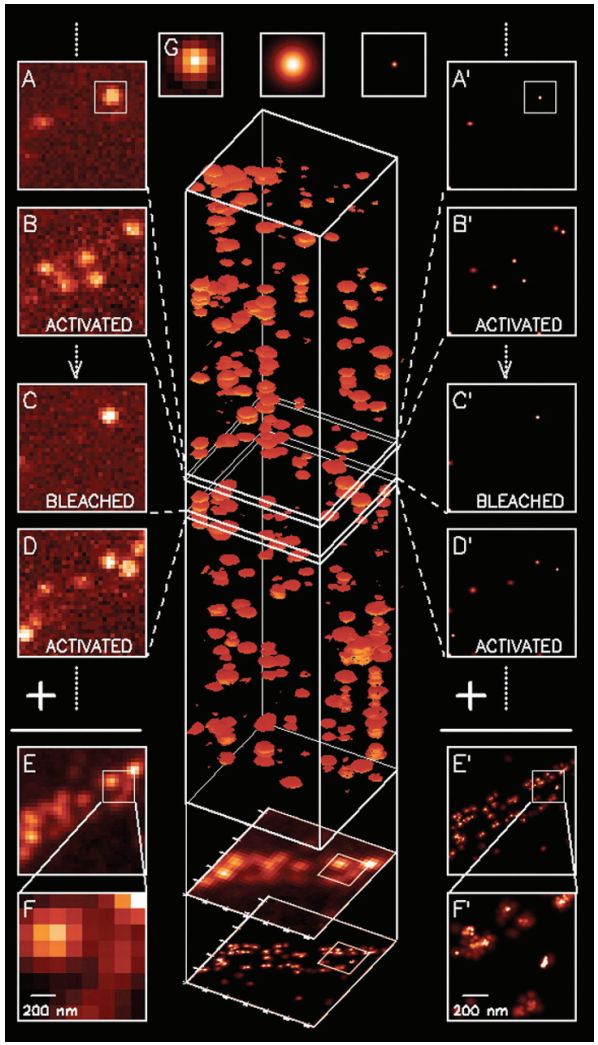

The principle behind PALM. A sparse subset of PA-FP molecules that are attached to proteins of interest and then fixed within a cell are activated (A and B) and then imaged until most are bleached (C). This process is repeated many times (C and D) until the population of inactivated, unbleached molecules is depleted. Summing the molecular images across all frames results in a diffraction-limited image (E and F). However, if the location of each molecule is first determined by fitting the expected molecular image given by the PSF of the microscope [(G), center] to the actual molecular image [(G), left], the molecule can be plotted [(G), right] as a Gaussian that has a standard deviation equal to the uncertainty s (x,y) in the fitted position. Repeating with all molecules across all frames (A' through D') and summing the results yields a superresolution image (E' and F') in which resolution is dictated by the uncertainties s(x,y) as well as by the density of localized molecules.

PALM

The principle behind PALM.

Central to the performance of photoactivated localization microscopy (PALM) is the precise localization of single fluorescent molecules performed by a least-squares fit of an assumed two-dimensional gaussian point spread function (PSF) to each single molecule image.

$$(\sigma_{x,y}{}^2)_m \approx \frac{s^2 + a^2/12}{N_m} + \frac{4\sqrt{\pi}s^3 b_m{}^2}{aN_m{}^2}$$

where s is the standard deviation of the PSF, a is the pixel size in the image (taking into account the system magnification), Nm is the total number of photons measured from molecule m, and bm is the number of background photons collected in the fitting windowused for molecule m.
Therefore, PALM design is predicated on achieving the highest possible diffraction limited resolution (i.e., small s) and collection efficiency (high Nm)consistent with minimal background noise bm .

The superresolution image resulting from the sum of all such rendered molecules thus provides a probability density map where brightness is proportional to the likelihood that a PA-FP molecule can be found at a given location.

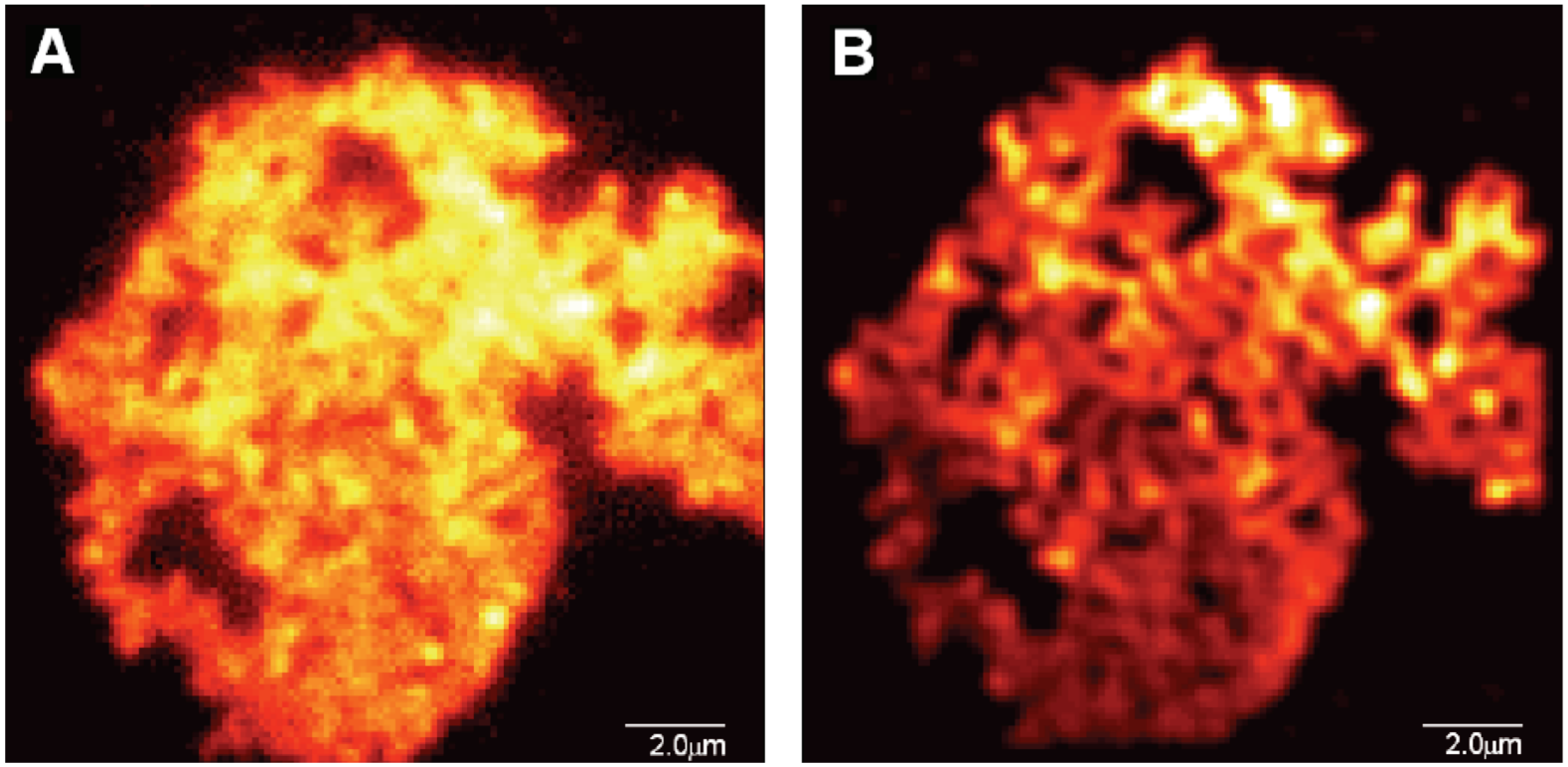

Images of an aggregation of 50 nm diameter plain polystyrene beads with the PA-FP Kaede deposited thereon. (A) Conventional TIRF image obtained prior to PALM data acquisition. (B) Summed TIRF image constructed by summing all the activated (red state), background-subtracted, diffraction-limited single molecule images in the entire PALM data stack.

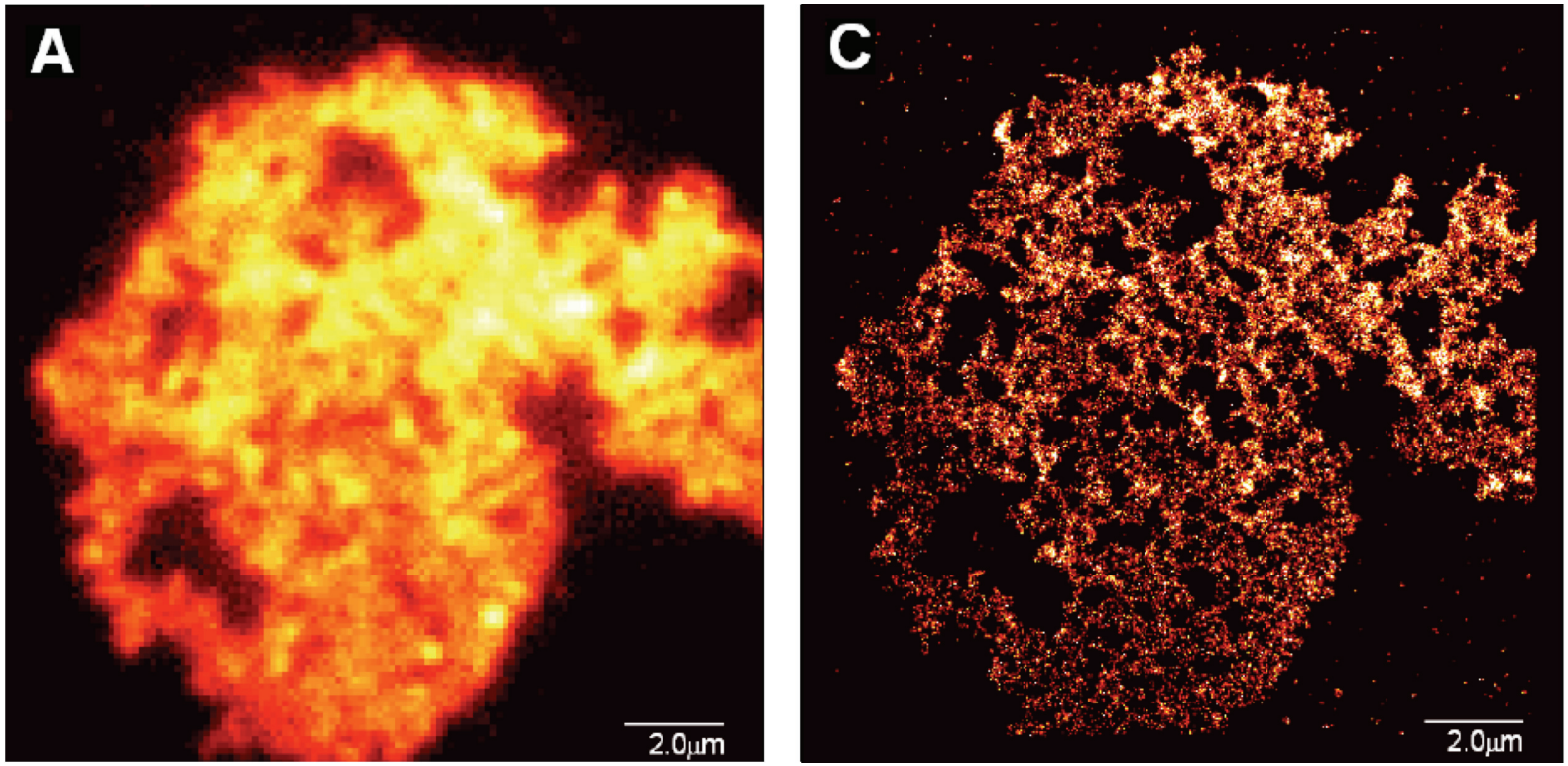

(C) PALM image constructed by summing the position probability gaussians determined for all localized molecules in the data stack.

Comparative summed-molecule TIRF (A) and PALM (B) images of the same region within a cryoprepared thin section from a COS-7 cell expressing the lysosomal transmembrane protein CD63 tagged with the PA-FP Kaede.

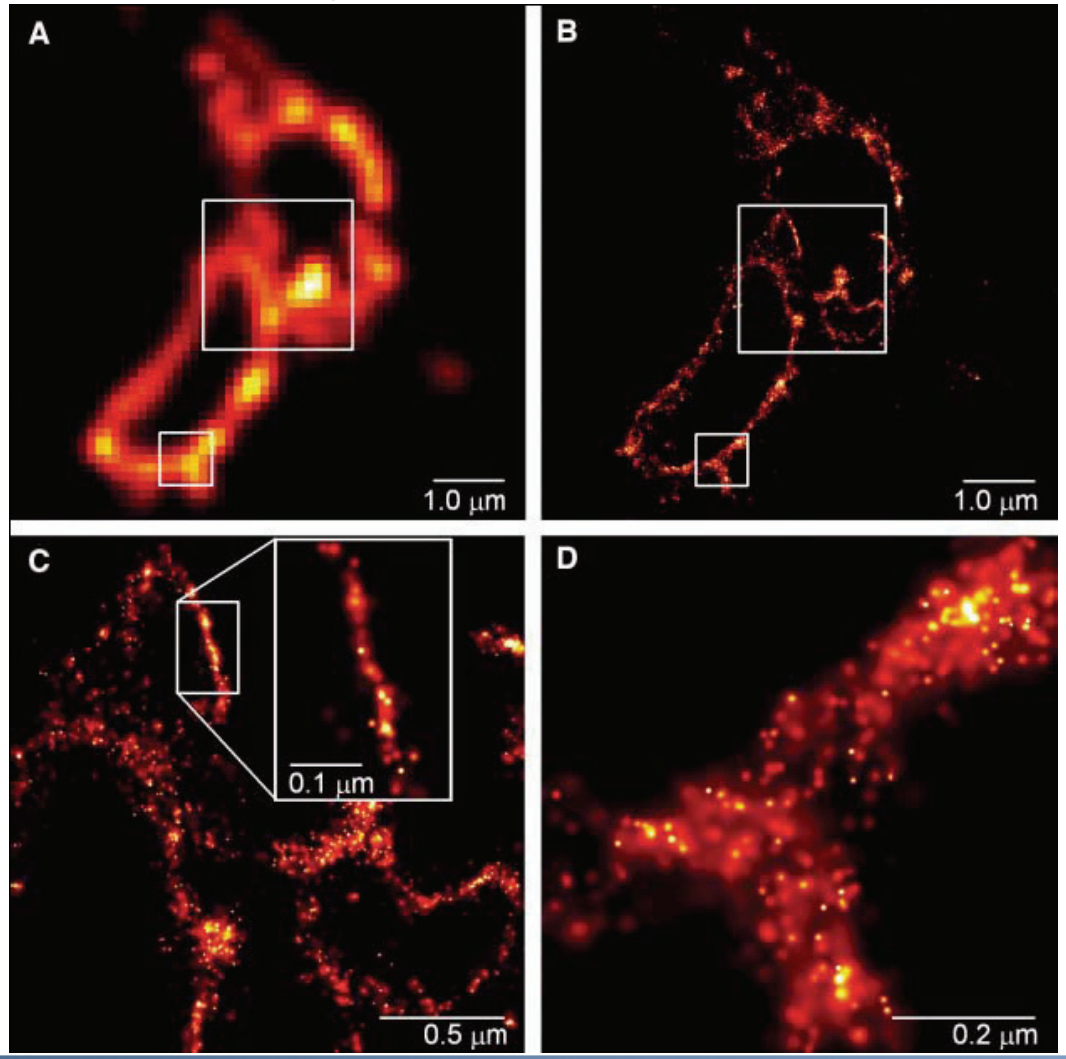

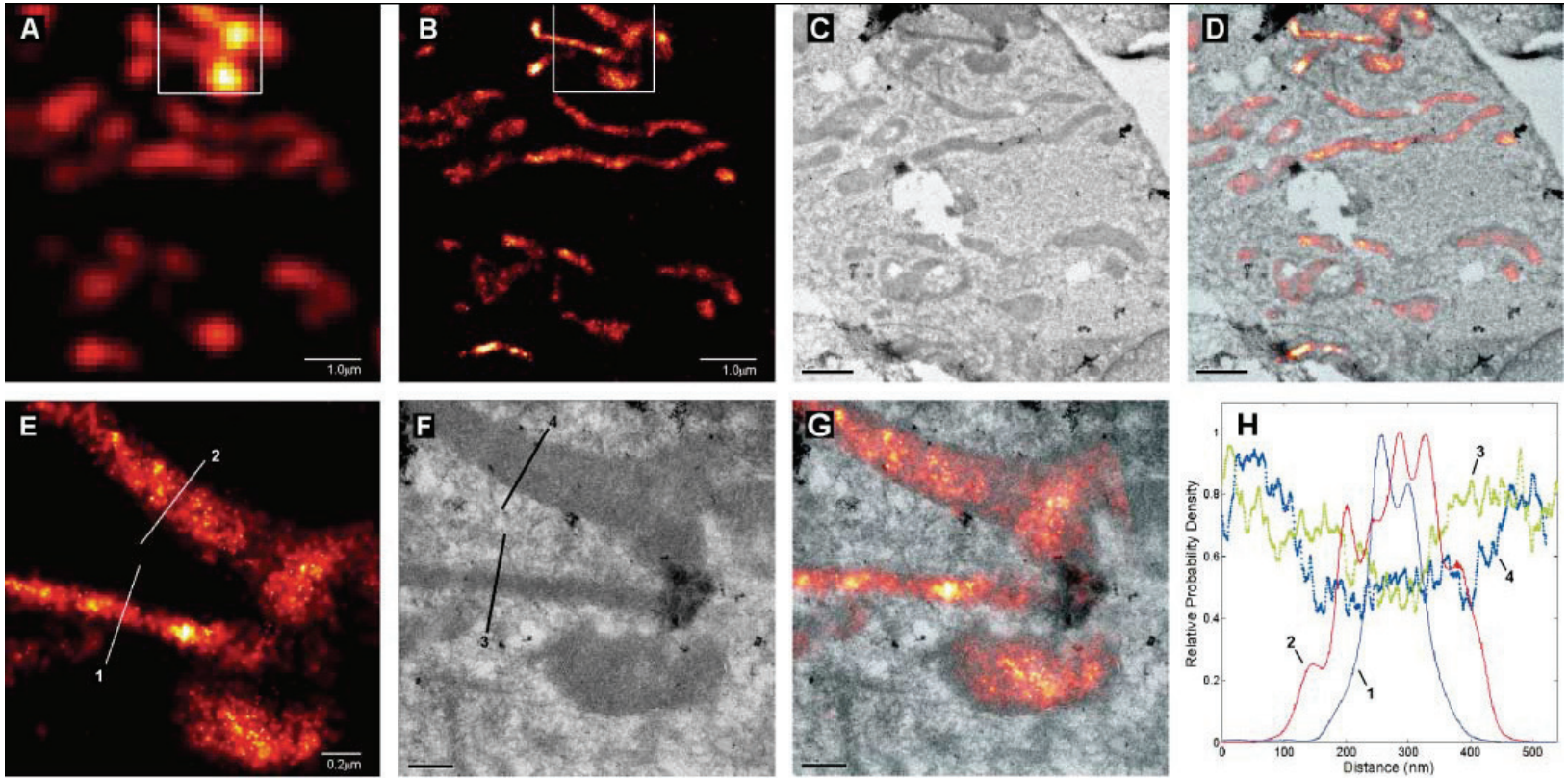

Comparative summed-molecule TIRF (A), PALM (B), TEM (C), and PALM/TEM overlay (D) images of mitochondria in a cryo-prepared thin section from a COS-7 cell expressing dEosFP-tagged cytochrome-C oxidase import sequence.

ULTIMATE RESOLUTION... AGAIN

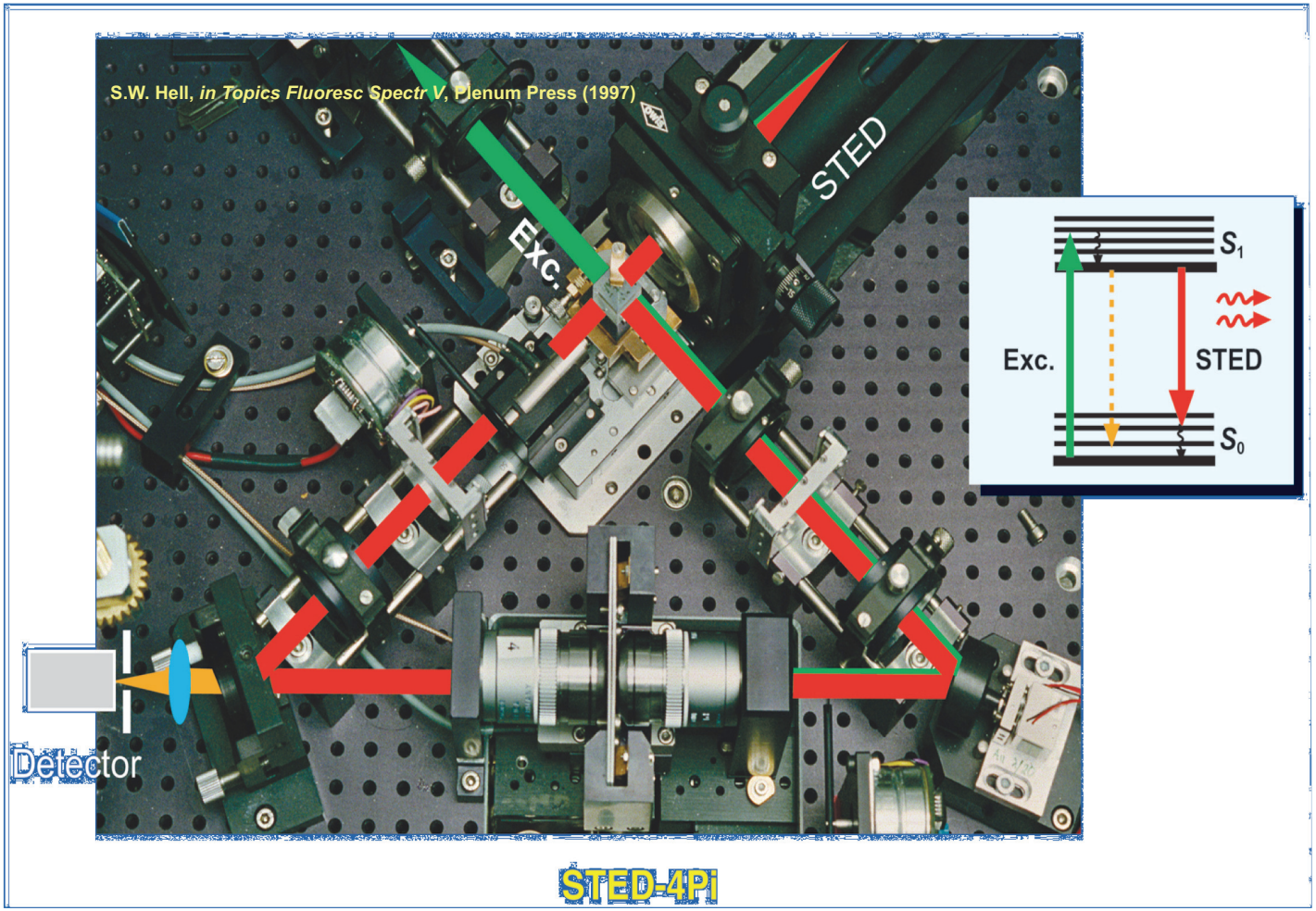

4PI AND STED

Dyba, M., Jakobs, S. & Hell, S.W. Immunofluorescence stimulated emission depletion microscopy. *Nat. Biotechnol.* **21**, 1303–1304 (2003).

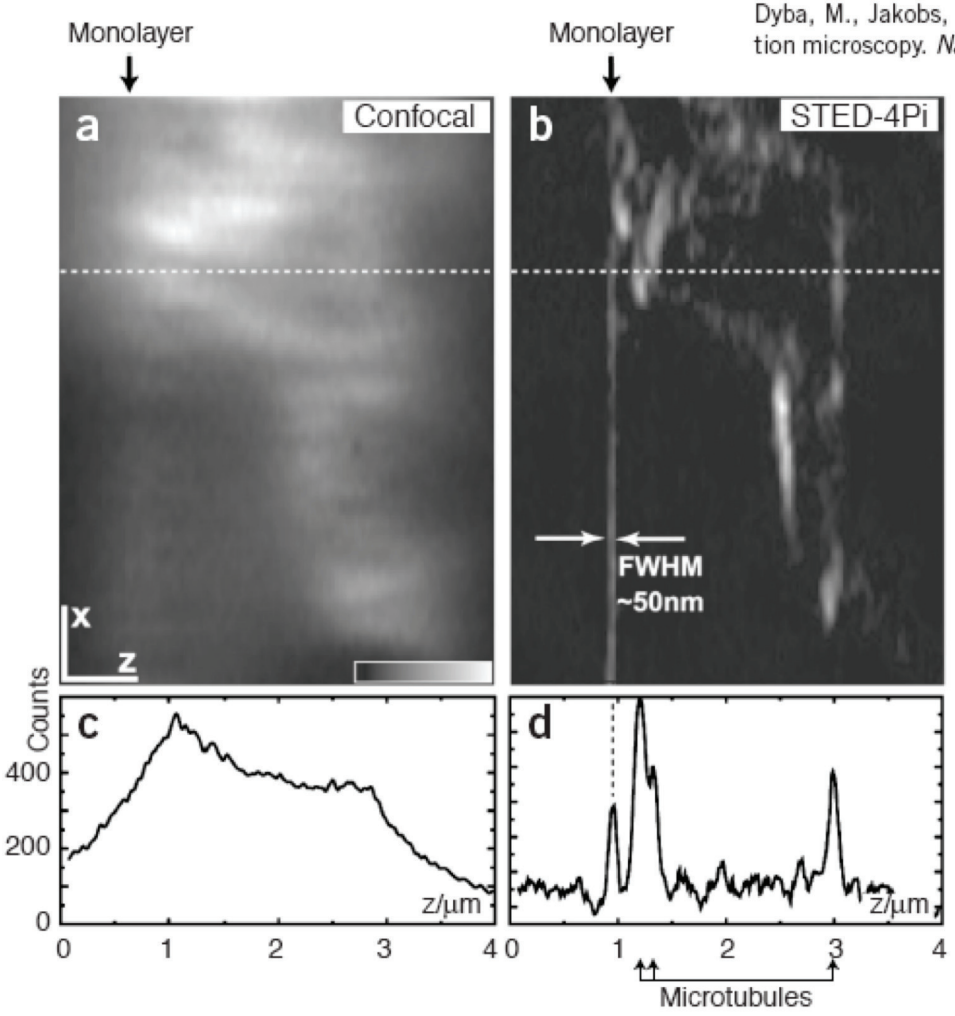

Microtubular network of human embryonic kidney cell against coverslip reference monolayer. Cells in water immersion geometry.

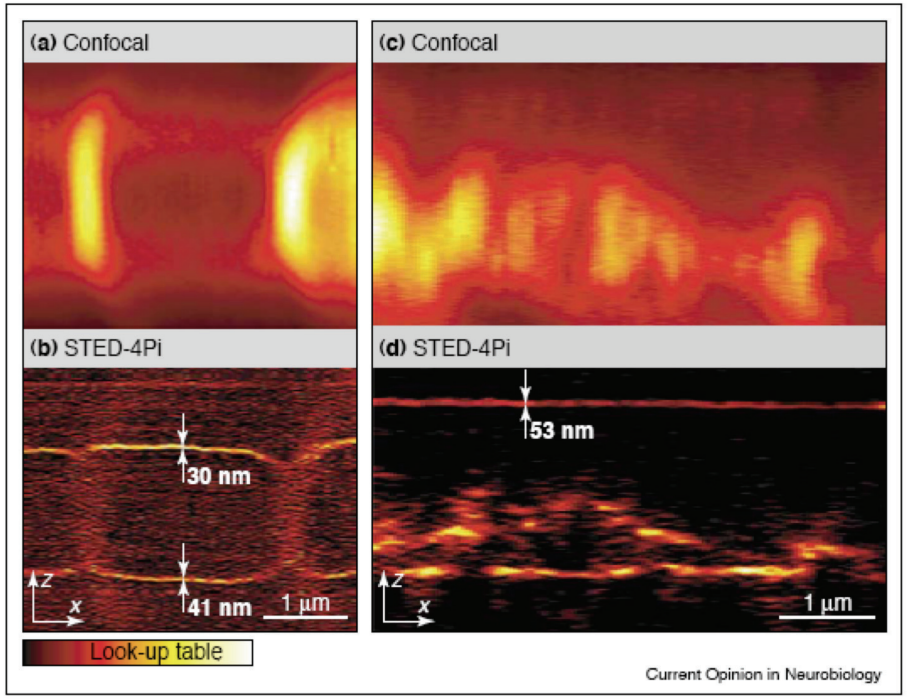

Axial resolution increase provided by STED-4Pi (b,d) over confocal microscopy (a,c). The membranes of a live bacterium (*Bacillus megaterium*) were stained with the dye RH 414 and then simultaneously imaged in the **(a)** confocal and in the **(b)** STED-4Pi microscopy mode. Note that the axial resolution of this focusing microscope is in the order of 30–40 nm. **(c,d)** xz-images from the immunolabeled microtubular network of a human embryonic kidney (HEK)-cell as recorded with a (c) confocal and (d) STED-4Pi-microscope. Both images have been recorded at the same site in the cell. The microtubules were labeled using a primary anti-β-tubulin antibody and a secondary antibody coupled to MR-121. The STED-4Pi images were linearly deconvolved to remove the effect of the 4Pi-sidelobes. Note the straight horizontal line which stems from an MR-121 layer on the cover slip. At this layer, the resolution in the STED-4Pi image is determined as 53 nm. The fixed HEK cells were mounted in aqueous buffer and recorded with water immersion lenses.

www.sciencedirect.com **Current Opinion in Neurobiology** 2004, **14**:599–609

ULTIMATE RESOLUTION... AGAIN

Sharpest focal spot

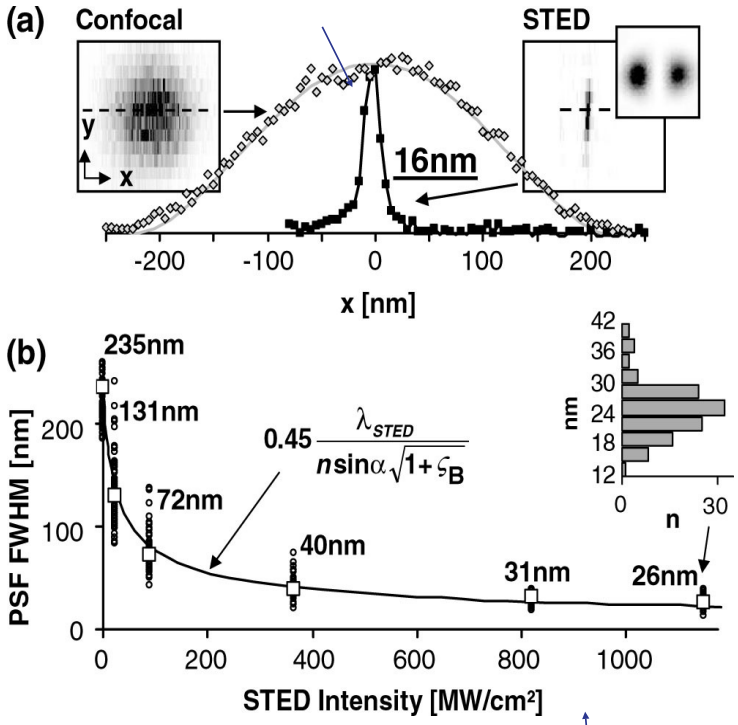

V. Westphal, S.W. Hell (2005). *Phys. Rev. Lett.* **94**, 143903.

Validation of A NEW square-root resolution law

MORE

Alberto Diaspro
Cesare Usai
Paola Ramoino
Partha P. Mondal
Giuseppe Vicidomini
Paolo Bianchini
Valentina Caorsi
Davide Mazza
Ilaria Testa
Francesca Cella
Emiliano Ronzitti
Silke Krol
Raffaella Magrassi
Marc Schneider
Munish Chanana
Mattia Pesce
Federica Morotti
Francesco Di Fato
Mirko Corosu

COMPAGNIA di San Paolo

fi difi

Università degli studi di Genova
Dipartimento di Fisica

IFOM

Festival della Scienza